Palestine Journal of Mathematics

Vol 15(1)(2026) , 487–516

A Fractional-Order Model for Hepatitis B Transmission in the Framework of Nonsingular and Nonlocal Kernel

Kaushal Soni and Arvind Kumar Sinha

Communicated by: Sunil Dutt Purohit

MSC(2020): 44A10, 46E39, 46N60, 92D30, 00A71.

Keywords: Atangana-Baleanu fractional derivative , Beddington-DeAngelis type incidence, Hepatitis B virus, Laplace transform, Mittag-Leffler.

Corresponding Author: Arvind Kumar Sinha

Abstract. Hepatitis B remains a major global health challenge, requiring advanced mathematical models to understand and control its spread. This study develops a fractional-order mathematical model using the Atangana-Baleanu fractional derivative in caputo sense (ABC), incorporating awareness, vaccination, and a Beddington-DeAngelis type incidence rate to better capture disease dynamics. The model considers preventive measures by susceptible individuals and the inhibition effect of treatment on infectives, providing a realistic approach to disease transmission. The study ensures the model's positivity and boundedness, demonstrates the existence and uniqueness of its solution, and investigates the Ulam-Hyers (UH) type stability and generlized Ulam-Hyers (GUH) type stability . It derives the Hepatitis B-free equilibrium (HBFE) and Hepatitis B-present equilibrium (HBPE) points, analyzing their local stability (LAS) using the basic reproduction number and proving the global stability (GAS) of the endemic equilibrium through a Lyapunov function. Sensitivity analysis identifies key parameters influencing disease transmission, offering valuable insights for control strategies. Numerical simulations use the Lagrange two-step polynomial method, effectively demonstrating parameter impacts on disease progression. The results show that higher awareness and vaccination rates reduce infection levels, emphasizing the role of public health interventions in controlling Hepatitis B. The study highlights the advantages of fractional-order modeling in capturing memory effects and long-term dependencies, offering a more precise approach than integer-order models. The findings provide a foundation for designing effective disease control policies and intervention strategies. This study presents a biologically relevant and mathematically rigorous model for Hepatitis B transmission. The proposed approach strengthens the case for fractional-order models in epidemiology, making it a valuable contribution to disease modeling and public health decision-making.

1 Introduction

HBV is a highly infectious disease that poses a significant health risk to populations across the globe. It is essential to recognize the severity of this sickness and take the required actions to avoid it. HBV poses a significant threat to liver health, capable of inflicting severe damage and potentially leading to dire consequences such as liver cancer and failure. In the early stages of

Hepatitis B, many people don't have any symptoms. However, some people suddenly start to feel sick and have symptoms like puking, skin turning yellow, tiredness, black pee, and stomach pain [1, 2]. A vaccine has been available since 1982 to protect against this illness. The vaccine has been tried and shown to stop the sickness 95% of the time [3]. HBV accounts for 80% of instances of primary liver cancer, and 25% of childhood diseases develop into chronic infections [4]. Most cases of HBV in countries with moderate to high endemicity occur via sexual contact, mother-to-child transmission, and percutaneous or other forms of contact with infected blood or bodily fluids [5, 6]. In 2015, there were around 900,000 fatalities caused by HBV infections. HBV is a recognized cause of major liver disorders such as cirrhosis and hepatocellular carcinoma. Birth immunization with Hepatitis B is one of the most efficient strategies to prevent the transfer of HBV from mother to child or via other means. Still, to lower the incidence rate, healthcare systems should do more to enhance their viral Hepatitis treatment and preventive programs. Lamivudine, telbivudine, and tenofovir are some of the antiviral medications that show promise in reducing the risk of perinatal HBV infection in pregnant women who have large amounts of HBV DNA [7, 8]. The dissemination of information on the risks of HBV infection and the significance of preventative techniques is greatly aided by media awareness campaigns. People may be informed about the dangers of HBV, particularly the fact that it can lead to cirrhosis and hepatocellular carcinoma (HCC), via extensive media campaigns that include commercials on television, radio, social media, and in print. The media has a unique opportunity to help communities combat the spread of HBV, especially from mother to child and other routes, by increasing public knowledge of the disease and encouraging people to take action. Another way that the media may help save lives and limit the spread of the HBV is by highlighting the need for Hepatitis B immunization at birth.

Mathematical modeling is useful in comprehending real-world problems, as shown in recent studies [9–14]. Mathematical models serve a crucial function in analyzing and controlling the transmission of contagious illnesses. The development of epidemic compartmental models by mathematicians and biologists around the world has been a major breakthrough in identifying how HBV spreads. These models serve as valuable tools for analyzing disease dynamics and assisting in the development of effective prevention and treatment strategies. Mathematical models using integer-order ordinary differential equations are often used to explore biological system dynamics [15, 16]. Many studies on HBV transmission dynamics and control have been published in recent decades. Nevertheless has only been utilized for classical differential equations of integer order, delay, or stochastic nature. Thornley et al. [17] formulated a model to examine the transmission dynamics of the HBV and proposed strategies for its control within the New Zealand population. Manna and Chakrabarty [18] investigated the stability of an HBV infection model by introducing one and two discrete delays. Anderson and May [19, 20] utilized a mathematical framework to demonstrate the impact of HBV transmission among carriers . Anderson and Williams provide models of transmission of Hepatitis-B by sexual activity [21]. Pang et al. [22] proposed a model to analyze the effects of vaccination and other control measures on HBV eradication. Zhao et al. [23] evaluated a model to determine the long-term effectiveness of vaccinations. Khan et al. [24] proposed a mathematical framework to analyze the influence of migration on HBV transmission.

To address the limitations of traditional integer-order models, researchers have increasingly turned to fractional calculus, which effectively captures non-local dynamics and complex behaviors in real-world systems. This has allowed for the emergence of important facts related to nature, which have been revealed through the use of fractional calculus [25, 26]. Fractional derivatives are the most suitable mathematical tool for studying epidemiological dynamical processes

that involve non-integer or fractional sequences and natural occurrences. Due to their memory-dependent nature, these structures effectively capture the complex dynamics of epidemiological systems involving multi-scale and non-linear interactions. Therefore, understanding the implications of memory effects on epidemiological processes is crucial for developing effective disease control strategies. Numerous scholars have explored epidemic models incorporating fractional operators for various communicable diseases, as these models exhibit a reasonable biphasic decline in disease transmission.

Many fractional-order derivatives have been developed and implemented across various disciplines [27–35]. In recent years, interest in fractional models has grown, as highlighted by author [36], who explains how fractional operators contribute to understanding their physical and geometric properties. Several researchers have developed and examined fractional-order HBV models within an epidemic framework [26, 37–39]. Meena et al. [40] conducted a novel investigation of the HBV using a fractional operator with a non-local kernel. Bhattar et al. [41] utilized the Hilfer fractional derivative in their analysis of HBV infection, offering a fractional-order perspective on disease dynamics. Habenom et al. [26] performed a numerical simulation to study the effects of vaccination and treatment in a fractional-order model of hepatitis B. Gour et al. [42] applied the homotopy decomposition method to analyze a fractional-order model of HBV infection. The Beddington DeAngelis type incidence rate, introduced by Beddington [43] and DeAngelis [44], is a nonlinear form given by $\frac{\beta \mathcal{S}\mathcal{J}}{1+k_1\mathcal{S}+k_2\mathcal{J}}$,where β is the transmission rate and k_1 and k_2 represent inhibition effects from the susceptible and infected populations, respectively. This form generalizes both bilinear and saturated incidence rates and provides a more realistic framework for modeling crowding effects and behavioral changes in HBV transmission dynamics [45, 46].

As far as we know, none of the available HBV models in the literature have constructed a fractional-order mathematical framework utilizing the ABC fractional derivative, integrating both an awareness parameter and a Beddington-DeAngelis type incidence rate to capture the intricate behavior of Hepatitis B spread and management.

This study is structured as follows:

Section 2 presents fundamental principles of fractional calculus. Section 3 describes the mathematical model in detail. Section 4 focuses on the qualitative analysis of the model. Section 5 explores the UH stability analysis. Section 6 discusses equilibrium points, their stability, and the basic reproduction number. Section 7 examines the sensitivity analysis. Section 8 model fitting and parameter estimation is performed. Section 9 outlines the numerical scheme used. Section 10 provides the discussion, conclusion, and potential future research directions.

2 Preliminary mathematical framework

This section begins with examining fundamental mathematical tools utilized in the following sections.

Definition 2.1 ([47]). Let $s \in [1, \infty)$ and O be an open subset of $\mathbb{R}$ The Sobolev space $H^s(O)$ is defined as: $H^s(O) = \{\mathscr{U} \in L^2(O) \ni \mathcal{D}^\tau \mathscr{U} \in L^2(O) \forall |\tau| \leqslant \mathfrak{g}\}$.

Using the aforementioned definition, Atangana and Baleanu [27] introduced the ABC fractional derivative.

Definition 2.2 ([27]). Let's introduce a function $\mathcal{F}(t) \in H^s(a, b)$ and a scalar $\tau \ni 0 < \tau < 1$; then ABC derivative given as:

$$ {}^{\mathscr{Q}}_{0}\mathfrak{D}^{\tau}_{t}\mathcal{F}(t) = \frac{\mathscr{Q}(\tau)}{(1-\tau)}\int_0^t \mathrm{E}_{\tau}\left(\frac{\tau}{\tau-1}(t-\rho)^{\tau}\right)\mathcal{F}'\mathrm{d}\rho, \tag{2.1} $$

where $\mathscr{Q}(\tau)$ represents a normalization mapping that satisfies the conditions $\mathscr{Q}(0) = \mathscr{Q}(1) = 1$.

Definition 2.3 ([27]). The usual definition of Laplace transformation (LT) of the function $\mathfrak{F}(t)$ is given by

$$ \mathrm{L}[\mathcal{F}(t), s] = \bar{\mathcal{F}}(s) = \int_0^{\infty} e^{-st}\mathcal{F}(t)\mathrm{d}t, \mathrm{R}(s) > \zeta, t \geqslant 0. \tag{2.2} $$

Inverse LT of $\bar{\mathcal{F}}(s)$ is given below

$$ \mathrm{L}^{-1}[\bar{\mathcal{F}}(s), t] = \frac{1}{2\pi i}\int_{\eta-i\infty}^{\eta+i\infty} e^{st}\bar{\mathcal{F}}(s)\mathrm{d}s, \text{where } \eta \in \mathbb{R}. \tag{2.3} $$

Definition 2.4 ([27]). Laplace transformation of ABC derivative define as :

$$ \mathrm{L}\left[{}^{\mathscr{Q}}_{0}\mathfrak{D}^{\tau}_{t}\mathcal{F}(t)\right] = \frac{\mathscr{Q}(\tau)}{1-\tau}\left[\frac{s^{\tau}\mathrm{L}\{\mathcal{F}(t)\} - s^{\tau-1}\mathcal{F}(0)}{s^{\tau} + \frac{\tau}{1-\tau}}\right]. \tag{2.4} $$

Definition 2.5 ([27]). Let's introduce a function $\mathcal{F}(t) \in \mathrm{H}^s(a, b)$ and a scalar τ such that $0 < \tau < 1$; then ABC derivative given as:

$$ {}^{\mathscr{Q}}_{0}\mathfrak{I}^{\tau}_{t}\mathcal{F}(t) = \frac{1-\tau}{\mathscr{Q}(\tau)}\mathcal{F}(t) + \frac{\tau}{\mathscr{Q}(\tau)\Gamma(\tau)}\int_0^t (t-\Psi)^{\tau-1}\mathcal{F}(\Psi)\mathrm{d}\Psi. \tag{2.5} $$

Definition 2.6 ([27]). The ML functions $\mathrm{E}_{\rho}(\mathfrak{Z})$ and $\mathrm{E}_{\rho,\tau}(\mathfrak{Z})$ were originally introduced by Mittag-Leffler and later generalized by Wiman.

$$ \mathrm{E}_{\rho}(\mathfrak{Z}) = \sum_{k=0}^{\infty}\frac{\mathfrak{Z}^k}{\Gamma(\rho k+1)}; (\mathfrak{Z}, \rho \in \mathbb{C}, \Re(\rho) > 0). \tag{2.6} $$

$$ \mathrm{E}_{\rho,\tau}(\mathfrak{Z}) = \sum_{k=0}^{\infty}\frac{\mathfrak{Z}^k}{\Gamma(\rho k+\tau)}; (\mathfrak{Z}, \rho, \tau \in \mathbb{C}, \Re(\rho) > 0, \Re(\tau) > 0). \tag{2.7} $$

Lemma 2.7 ([48]). *The solution to the given problem for* $0 < \tau \leqslant 1$,

$$ {}^{\mathscr{Q}}_{0}\mathfrak{D}^{\tau}_{t}\mathcal{F}(t) = \mathscr{G}(t),\ t \in [0, \eth],\ \mathcal{F}(0) = \mathcal{F}_0. \tag{2.8} $$

where $\mathcal{F} : [0, \eth] \to \mathbb{R}$ *is a function* $\mathcal{F}_0$ *is a fixed point define by*

$$ \mathcal{F}(t) = \mathcal{F}_0 + \frac{1-\tau}{\mathscr{Q}(\tau)}\mathscr{G}(t) + \frac{\tau}{\mathscr{Q}(\tau)\Gamma(\tau)}\int_0^t (t-\Psi)^{\tau-1}\mathscr{G}(\Psi)\mathrm{d}\Psi. \tag{2.9} $$

Lemma 2.8 ([49]). *Let* $\mathfrak{F}(t) \in \mathbb{R}$ *be a function that is continuous and differentiable. Then for each* $t \geqslant t_0$

$$ \frac{1}{2}\,{}^{\mathscr{Q}}_{t_0}\mathfrak{D}^{\tau}_{t}\mathfrak{F}^2(t) \leqslant \mathfrak{F}(t)\,{}^{\mathscr{Q}}_{t_0}\mathfrak{D}^{\tau}_{t}\mathfrak{F}(t),\ \forall\tau \in (0,1). \tag{2.10} $$

Theorem 2.9 (Krasnoselskii's fixed point theorem [50]). *Let* $\mathcal{Z}_q \neq \phi$ *, closed, convex, and bounded subset of a Banach space* $\aleph$. *Suppose that and* $\mathscr{U}$ *and* $\mathscr{W}$ *are two operators defined on* $\aleph$ *that satisfy the following conditions:*

(i) $\mathscr{U}(\mathscr{G}) + \mathscr{W}(\mathscr{G}) \in \mathcal{Z}_q, \forall \mathscr{G} \in \mathcal{Z}_q$,

(ii) $\mathscr{U}$ *is a mapping that satisfies the contraction property,*

(iii) $\mathscr{W}$ *is a compact and continuous operator.*

Consequently, at least one solution $\mathscr{G}$ *can be found in* $\mathcal{Z}_q$ *such that* $\mathscr{U}(\mathscr{G}) + \mathscr{W}(\mathscr{G}) = \mathscr{G}$ *holds.*

Theorem 2.10 (Arzela-Ascoli theorem [51]). *This theorem states that for a compact set* $\mathcal{Z}_q$ *in* $\mathbb{R}^n$*, a subset* Y *of* $C(\mathcal{Z}_q)$ *is relatively compact in* $C(\mathcal{Z}_q) \iff$ *the functions in* Y *are uniformly bounded and equicontinuous on* $\mathcal{Z}_q$.

3 Model formulation

We constructed a mathematical model for HBV utilizing ABC derivatives, where the total population is divided into three categories: Susceptible $(\widehat{\mathcal{S}})$, Infected $(\widehat{\mathcal{I}})$, and Recovered $(\widehat{\mathcal{R}})$. The model incorporates a constant recruitment rate for the susceptible population and an incidence rate governed by the Beddington-DeAngelis type $(1-\zeta)\frac{\beta\widehat{\mathcal{S}}\widehat{\mathcal{I}}}{1+k_1\widehat{\mathcal{S}}+k_2\widehat{\mathcal{I}}}$. In the model, ζ is rate of awareness programs and k_1 represents the effect of preventive measures by susceptible individuals, while k_2 accounts for the reduction in transmission due to the impact of the infected population, including crowding and protective behaviors. Additionally, we consider that some infected individuals with sufficient physical resilience can recover naturally without medical intervention. During an epidemic, various social platforms play a crucial role in disseminating information about disease symptoms, preventive measures, and treatment options through media such as television, radio, and educational campaigns. Public awareness encourages individuals to adopt protective measures.

The HBV model is structured as follows:

$$\begin{aligned}
{}^{\mathscr{D}}_{0}\mathfrak{D}^{\tau}_{t}\widehat{\mathcal{S}}(t) &= \theta - (1-\zeta)\frac{\beta\widehat{\mathcal{S}}\widehat{\mathcal{I}}}{1+k_1\widehat{\mathcal{S}}+k_2\widehat{\mathcal{I}}} - (\mu+m)\widehat{\mathcal{S}},\\
{}^{\mathscr{D}}_{0}\mathfrak{D}^{\tau}_{t}\widehat{\mathcal{I}}(t) &= (1-\zeta)\frac{\beta\widehat{\mathcal{S}}\widehat{\mathcal{I}}}{1+k_1\widehat{\mathcal{S}}+k_2\widehat{\mathcal{I}}} - (\mu+\delta+\eta)\widehat{\mathcal{I}},\\
{}^{\mathscr{D}}_{0}\mathfrak{D}^{\tau}_{t}\widehat{\mathcal{R}}(t) &= \eta\widehat{\mathcal{I}} + m\widehat{\mathcal{S}} - \mu\widehat{\mathcal{R}}.
\end{aligned} \tag{3.1}$$

Table 1 provides the details of the parameters.

Table 1: Description of model parameters.

Parameter	Description (with units)
β	Transmission rate of the disease (per person per day)
η	Recovery rate of infected individuals (per day)
τ	Fractional-order parameter controlling memory effects (dimensionless)
μ	Natural death rate of individuals (per day)
θ	Recruitment rate into the population (individuals per day)
ζ	Rate of awareness program implementation (per day)
k_1, k_2	Saturation factors representing behavioral inhibition (dimensionless)
δ	Disease-induced death rate (per day)
m	Transformation rate from susceptible to recovred (per day)

4 Qualitative analysis

Since model (3.1) represents a community of individuals, it is crucial to determine the domain where it remains epidemiologically relevant.

Theorem 4.1. *Lets consider closed set* $\widehat{\mho} = \left\{(\widehat{\mathcal{S}}, \widehat{\mathcal{I}}, \widehat{\mathcal{R}}) \in \mathbb{R}^3_+ : \widehat{\mathcal{N}} = \widehat{\mathcal{S}} + \widehat{\mathcal{I}} + \widehat{\mathcal{R}} \leqslant \frac{\theta}{\mu}\right\}$ *remains positively invariant for model (3.1).*

Proof. Summing all the equations of the fractional model (3.1) yields the following result.

$$ {}^{\mathscr{Q}}_{0}\mathfrak{D}^{\tau}_{t}\widehat{\mathcal{N}}(t) \leqslant \theta - \mu\widehat{\mathcal{N}}. \tag{4.1}$$

After applying the LT and simplifying, we derive the following outcome.

$$\begin{aligned} &\frac{\mathscr{Q}(\tau)}{1-\tau}\left[\frac{s^{\tau}\mathcal{L}(\widehat{\mathcal{N}}(t)) - s^{\tau-1}\widehat{\mathcal{N}}(0)}{s^{\tau} + \frac{\tau}{1-\tau}}\right] \leqslant \frac{\theta}{s} - \mu\mathcal{L}(\widehat{\mathcal{N}}(t)), \\ &\frac{\mathscr{Q}(\tau)}{1-\tau}\left[\frac{s^{\tau}\mathcal{L}(\widehat{\mathcal{N}}(t))}{s^{\tau} + \frac{\tau}{1-\tau}}\right] + \mu\mathcal{L}(\widehat{\mathcal{N}}(t) \leqslant \frac{\theta}{s} + \frac{\mathscr{Q}(\tau)s^{\tau-1}\widehat{\mathcal{N}}(0)}{s^{\tau}(1-\tau)+\tau}. \end{aligned} \tag{4.2}$$

After simplify we get:

$$\mathcal{L}(\widehat{\mathcal{N}}(t)) \leqslant \frac{\theta}{s}\left(\frac{s^{\tau}(1-\tau)+\tau}{\mathscr{Q}(\tau)s^{\tau} + \mu(s^{\tau}(1-\tau)+\tau)}\right) + \frac{\mathscr{Q}(\tau)\widehat{\mathcal{N}}(0)s^{\tau-1}}{\mathscr{Q}(\tau)s^{\tau} + \mu(s^{\tau}(1-\tau)+\tau)}. \tag{4.3}$$

Taking inverse LT in Equation (4.3) then we get:

$$\begin{aligned} \widehat{\mathcal{N}}(t) \leqslant{}& \frac{\theta\tau t^{\tau}}{\mathscr{Q}(\tau)+\mu(1-\tau)}\mathrm{E}_{\tau,\tau+1}\left(-\frac{\mu\tau t^{\tau}}{\mathscr{Q}(\tau)+\mu(1-\tau)}\right) \\ &+ \left(\frac{\theta(1-\tau)}{\mathscr{Q}(\tau)+\mu(1-\tau)} + \frac{\widehat{\mathcal{N}}(0)\mathscr{Q}(\tau)}{\mathscr{Q}(\tau)+\mu(1-\tau)}\right)\mathrm{E}_{\tau,1}\left(-\frac{\mu\tau t^{\tau}}{\mathscr{Q}(\tau)+\mu(1-\tau)}\right). \end{aligned} \tag{4.4}$$

Furthermore,

$$\mathrm{E}_{\tau,\tau+1}\left(-\frac{\mu\tau t^{\tau}}{\mathscr{Q}(\tau)+\mu(1-\tau)}\right) = \frac{1}{\left(-\frac{\mu\tau t^{\tau}}{\mathscr{Q}(\tau)+\mu(1-\tau)}\right)}\left[\mathrm{E}_{\tau,1}\left(-\frac{\mu\tau t^{\tau}}{\mathscr{Q}(\tau)+\mu(1-\tau)}\right)+1\right]. \tag{4.5}$$

Thus

$$\begin{aligned} \widehat{\mathcal{N}}(t) \leqslant{}& \frac{\theta\tau t^{\tau}}{\mathscr{Q}(\tau)+\mu(1-\tau)}\frac{1}{\left(-\frac{\mu\tau t^{\tau}}{\mathscr{Q}(\tau)+\mu(1-\tau)}\right)}\left[\mathrm{E}_{\tau,1}\left(-\frac{\mu\tau t^{\tau}}{\mathscr{Q}(\tau)+\mu(1-\tau)}\right)+1\right] \\ &+ \left(\frac{\widehat{\mathcal{N}}(0)\mathscr{Q}(\tau)}{\mathscr{Q}(\tau)+\mu(1-\tau)}\right)\mathrm{E}_{\tau,1}\left(-\frac{\mu\tau t^{\tau}}{\mathscr{Q}(\tau)+\mu(1-\tau)}\right). \end{aligned} \tag{4.6}$$

Utilizing the asymptotic properties of the ML function [52], we derive $\widehat{\mathcal{N}}(t) \to \frac{\theta}{\mu}$ as $t \to \infty$. Consequently, the solutions to system (3.1) for the Hepatitis B model are bounded ($\widehat{\mathcal{N}} \leqslant \frac{\theta}{\mu}$).

The condition $\widehat{\mathcal{N}} \leqslant \frac{\theta}{\mu}$. Biologically represents a demographic carrying capacity that is, the maximum population size that can be naturally sustained over time under constant birth and death

rates. This concept of carrying capacity ensures that the model remains realistic and biologically feasible by preventing the possibility of uncontrolled population growth.
Now we established positivity of the solution of the model (3.1). The first equation of the system (3.1) can be expressed as:

$$
\begin{aligned}
&{}_{0}^{\mathscr{Q}}\mathfrak{D}_{t}^{\tau}\widehat{\mathcal{S}}(t) = \theta - (1-\tau)\frac{\beta\widehat{\mathcal{S}}\widehat{\mathcal{I}}}{1+k_1\widehat{\mathcal{S}}+k_2\widehat{\mathcal{I}}} - (\mu+m)\widehat{\mathcal{S}},\\
&{}_{0}^{\mathscr{Q}}\mathfrak{D}_{t}^{\tau}\widehat{\mathcal{S}}(t) \geqslant -(\mu+m)\widehat{\mathcal{S}},
\end{aligned}
$$

taking LT, then we get

$$
\frac{\mathscr{Q}(\tau)}{1-\tau}\left[\frac{s^{\tau}\mathcal{L}(\widehat{\mathcal{S}}(t)) - s^{\tau-1}\widehat{\mathcal{S}}(0)}{s^{\tau}+\frac{\tau}{1-\tau}}\right] \geqslant -(\mu+m)\mathcal{L}(\widehat{\mathcal{S}}(t)),
$$

after simplification we get obtains

$$
\widehat{\mathcal{S}}(t) \geqslant \frac{\widehat{\mathcal{S}}(0)}{1+(\mu+m)(1-\tau)}\left[t^{\tau-1}E_{\tau,1}\left(\frac{-(\mu+m)\tau t}{1+(\mu+m)(1-\tau)}\right)\right].
$$

Thus, as $t \to \infty$, we have $\widehat{\mathcal{S}}(t) \geqslant 0$. As well as $\widehat{\mathcal{I}}(t) \geqslant 0$ and $\widehat{\mathcal{R}}(t) \geqslant 0$. Any solution of the fractional model (3.1) that starts with non-negative initial values in $\widehat{\upsilon}$ will persist within $\widehat{\upsilon}$ for all time. Hence, the closed set $\widehat{\upsilon}$ is preserved as positively invariant within the fractional model (3.1).

□

4.1 Existence and uniqueness

In this section, we explore the qualitative aspects of the proposed fractional system (3.1) for Hepatitis B. To do so, we begin by introducing

$$
\begin{cases}
{}_{0}^{\mathscr{Q}}\mathfrak{D}_{t}^{\tau}\widehat{\mathcal{S}}(t) = \mathcal{M}_1(t,\widehat{\mathcal{S}},\widehat{\mathcal{I}},\widehat{\mathcal{R}}),\\
{}_{0}^{\mathscr{Q}}\mathfrak{D}_{t}^{\tau}\widehat{\mathcal{I}}(t) = \mathcal{M}_2(t,\widehat{\mathcal{S}},\widehat{\mathcal{I}},\widehat{\mathcal{R}}),\\
{}_{0}^{\mathscr{Q}}\mathfrak{D}_{t}^{\tau}\widehat{\mathcal{R}}(t) = \mathcal{M}_3(t,\widehat{\mathcal{S}},\widehat{\mathcal{I}},\widehat{\mathcal{R}}),
\end{cases}
\tag{4.7}
$$

where

$$
\begin{cases}
\mathcal{M}_1(t,\widehat{\mathcal{S}},\widehat{\mathcal{I}},\widehat{\mathcal{R}}) = \theta - (1-\zeta)\frac{\beta\widehat{\mathcal{S}}\widehat{\mathcal{I}}}{1+k_1\widehat{\mathcal{S}}+k_2\widehat{\mathcal{I}}} - (\mu+m)\widehat{\mathcal{S}},\\
\mathcal{M}_2(t,\widehat{\mathcal{S}},\widehat{\mathcal{I}},\widehat{\mathcal{R}}) = (1-\zeta)\frac{\beta\widehat{\mathcal{S}}\widehat{\mathcal{I}}}{1+k_1\widehat{\mathcal{S}}+k_2\widehat{\mathcal{I}}} - (\mu+\delta+\eta)\widehat{\mathcal{I}},\\
\mathcal{M}_3(t,\widehat{\mathcal{S}},\widehat{\mathcal{I}},\widehat{\mathcal{R}}) = \eta\widehat{\mathcal{I}} + m\widehat{\mathcal{S}} - \mu\widehat{\mathcal{R}},
\end{cases}
\tag{4.8}
$$

which can be expressed as:

$$
\begin{cases}
{}_{0}^{\mathscr{Q}}\mathfrak{D}_{t}^{\tau}\mathscr{G}(t) = \mathcal{M}(t,\mathscr{G}(t)), t \in K = [0,T],\\
\mathcal{M}(0) = \mathcal{M}_0\ 0 < \tau \leqslant 0,
\end{cases}
\tag{4.9}
$$

where

$$\mathscr{G}(t) = \begin{pmatrix} \widehat{\mathcal{S}}(t) \\ \widehat{\mathcal{I}}(t) \\ \widehat{\mathcal{R}}(t) \end{pmatrix}, \quad \mathscr{G}(0) = \begin{pmatrix} \widehat{\mathcal{S}}(0) \\ \widehat{\mathcal{I}}(0) \\ \widehat{\mathcal{R}}(0) \end{pmatrix}, \quad \mathcal{M}(t, \mathscr{G}(t)) = \begin{pmatrix} \mathcal{M}_1(t, \widehat{\mathcal{S}}, \widehat{\mathcal{I}}, \widehat{\mathcal{R}}) \\ \mathcal{M}_2(t, \widehat{\mathcal{S}}, \widehat{\mathcal{I}}, \widehat{\mathcal{R}}) \\ \mathcal{M}_3(t, \widehat{\mathcal{S}}, \widehat{\mathcal{I}}, \widehat{\mathcal{R}}) \end{pmatrix}. \tag{4.10}$$

From lemma (2.7) the fractional initial value problem (IVP) (4.9) has a solution that can be represented by a nonlinear Volterra-type integral equation.

$$\mathscr{G}(t) = \mathscr{G}(0) + \frac{1-\tau}{\mathscr{Q}(\tau)}\mathcal{M}(t, \mathscr{G}(t)) + \frac{\tau}{\mathscr{Q}(\tau)\Gamma(\tau)}\int_0^t (t-\psi)^{\tau-1}\mathcal{M}(\psi, \mathscr{G}(t))\,d\psi. \tag{4.11}$$

Thus, examining whether a unique solution exists for the fractional HBV model (3.1), which has been reformulated as the fractional initial value problem (IVP) (4.9), is equivalent to analyzing the existence and uniqueness of solutions for the corresponding nonlinear integral equation (5.7). To achieve this, we define the Banach space $\aleph = C(K, \mathbb{R}^3_+)$ under the supremum norm.

$$\|\mathscr{G}(t)\| = \sup_{t\in K}\{|\mathscr{G}(t)| : \mathscr{G} \in \aleph\},$$

where

$$\sup_{t\in K}|\mathscr{G}(t)| = \sup_{t\in K}\left[|\widehat{\mathcal{S}}(t)| + |\widehat{\mathcal{I}}(t)| + |\widehat{\mathcal{R}}(t)|\right],$$

and $\widehat{\mathcal{S}}(t), \widehat{\mathcal{I}}(t), \widehat{\mathcal{R}}(t) \in C(K, \mathbb{R}_+)$. We define an operator $\Pi : \aleph \to \aleph$ as:

$$\Pi[\mathscr{G}(t)] = \mathscr{U}[\mathscr{G}(t)] + \mathscr{W}[\mathscr{G}(t)], \tag{4.12}$$

where

$$\mathscr{U}[\mathscr{G}(t)] = \mathscr{G}(0) + \frac{1-\tau}{\mathscr{Q}(\tau)}\mathcal{M}(t, \mathscr{G}(t)), \tag{4.13}$$

and

$$\mathscr{W}[\mathscr{G}(t)] = \frac{\tau}{\mathscr{Q}(\tau)\Gamma(\tau)}\int_0^t (t-\psi)^{\tau-1}\mathcal{M}(\psi, \mathscr{G}(t))\,d\psi. \tag{4.14}$$

The fractional integral equation (5.7) can be expressed in the form of a fixed-point problem.

$$\mathscr{G}(t) = \Pi[\mathscr{G}(t)]. \tag{4.15}$$

We apply the Lipschitz criterion to analyze our proposed system as follows:

Theorem 4.2. *The function* $\mathcal{M} : K \times \mathbb{R}^3_+ \to \mathbb{R}^3_+$ *is an fulfills the Lipschitz criterion* $\|\mathcal{M}(t, \mathscr{G}(t)) - \mathcal{M}(t, \widehat{\mathscr{G}}(t))\| \leqslant \mathfrak{K}_1\|\mathscr{G}(t) - \widehat{\mathscr{G}}(t)\|$ *for some* $\mathfrak{K}_1 \geqslant 0$.

Proof. Let $\mathscr{G}(t), \widehat{\mathscr{G}}(t) \in \aleph$

$$\begin{aligned} \|\mathcal{M}_1(t, \mathscr{G}(t)) - \mathcal{M}_1(t, \widehat{\mathscr{G}}(t))\| &= \|\theta - (1-\zeta)\frac{\beta\widehat{\mathcal{S}}\widehat{\mathcal{I}}}{1 + k_1\widehat{\mathcal{S}} + k_2\widehat{\mathcal{I}}} - (\mu + m)\widehat{\mathcal{S}} \\ &\quad - (\theta - (1-\zeta)\frac{\beta\widehat{\mathcal{S}}_1\widehat{\mathcal{I}}}{1 + k_1\widehat{\mathcal{S}}_1 + k_2\widehat{\mathcal{I}}} - (\mu + m)\widehat{\mathcal{S}}_1)\| \\ &\leqslant \mathfrak{Y}_1\|\widehat{\mathcal{S}} - \widehat{\mathcal{S}}_1\|, \end{aligned}$$

where $\mathfrak{Y}_1 = \mathfrak{w}_1 + (\mu + \mathfrak{m}),\ \|(1-\zeta)\frac{\beta\widehat{\mathcal{J}}}{1+k_1\widehat{\mathcal{S}}+k_2\widehat{\mathcal{J}}}\| \leqslant \mathfrak{w}$.

Similarly we can proof that

$$\|\mathcal{M}_2(t,\mathscr{G}(t)) - \mathcal{M}_2(t,\widehat{\mathscr{G}}(t))\| \leqslant \mathfrak{Y}_2\|\widehat{\mathcal{J}} - \widehat{\mathcal{J}}_1\|,$$

$$\|\mathcal{M}_3(t,\mathscr{G}(t)) - \mathcal{M}_3(t,\widehat{\mathscr{G}}(t))\| \leqslant \mathfrak{Y}_3\|\widehat{\mathcal{R}} - \widehat{\mathcal{R}}_1\|,$$

where $\mathfrak{Y}_2 = \mathfrak{w}_2 + (\mu + \delta + \eta),\ \|(1-\zeta)\frac{\beta\widehat{\mathcal{S}}}{1+k_1\widehat{\mathcal{S}}+k_2\mathcal{J}}\| \leqslant \mathfrak{w}_2$, and $\mathfrak{Y}_2 = \mu$.

Now we obtain

$$\begin{aligned}\|\mathcal{M}(t,\mathscr{G}(t)) - \mathcal{M}(t,\widehat{\mathscr{G}}(t))\| &\leqslant \mathfrak{Y}_1\|\mathcal{S} - \mathcal{S}_1\| + \mathfrak{Y}_2\|\mathcal{J} - \mathcal{J}_1\| + \mathfrak{Y}_3\|\mathcal{R} - \mathcal{R}_1\| \\ &\leqslant \mathfrak{K}_1\|\mathscr{G}(t) - \widehat{\mathscr{G}}(t)\|.\end{aligned}$$

Let $\mathfrak{K}_1 = \max\{\mathfrak{Y}_1, \mathfrak{Y}_2, \mathfrak{Y}_3\}$ hence $\mathcal{M}(t,\mathscr{G}(t))$ is satisfied Lipschitz condition.

□

Moreover, we assume that the nonlinear function $\mathcal{M} : K \times \mathbb{R}^3_+ \to \mathbb{R}^3_+$, presented in equation (5.7), adheres to t the linear growth constraint.

(i) There exist two positive constant $\mathfrak{K}_2,\ \mathfrak{K}_3 \ni$

$$\|\mathcal{M}(t,\mathscr{G})\| \leqslant \mathfrak{K}_2\|\mathscr{G}(t)\| + \mathfrak{K}_3, t \in K, \mathscr{G} \in \aleph. \tag{4.16}$$

Theorem 4.3. *Consider the fractional HBV model represented by equation (3.1) in the form of equation (4.9). Given the Theorem (4.2) and assumption (i), the associated integral equation (5.7) has at least one solution. Therefore, the proposed model (3.1) possesses at least one solution.*

Proof. Let $\mathcal{Z}_q$ be a closed covex bounded subset of $\aleph$ defined as $\mathcal{Z}_q = \{\mathscr{G} \in \aleph : \|\mathscr{G}\| \leqslant q, q > 0\}$,
where $q \geqslant \frac{\Upsilon_1}{1-\Upsilon_2}$, where

$$\Upsilon_1 = \mathscr{G}(0) + \left[\frac{1-\tau}{\mathscr{Q}(\tau)} + \frac{T^\tau}{\mathscr{Q}(\tau)\Gamma(\tau)}\right]\mathfrak{K}_3, \text{ and } \quad \Upsilon_2 = \left[\frac{1-\tau}{\mathscr{Q}(\tau)} + \frac{T^\tau}{\mathscr{Q}(\tau)\Gamma(\tau)}\right]\mathfrak{K}_2.$$

The proof of the theorem is structured into the following three steps.

Step I: First, we demonstrate that $\Pi[\mathscr{G}(t)] = \mathscr{U}[\mathscr{G}(t)] + \mathscr{W}[\mathscr{G}(t)] \in \mathcal{Z}_q$, for $t \in K$ and $\mathscr{G} \in \mathcal{Z}_q$. In fact, based on assumption (i), we obtain the following result.

$$\Pi[\mathcal{G}(t)] \leqslant \operatorname*{Sup}_{t\in K}\left\{\mathcal{G}(0)+\frac{1-\tau}{\mathcal{Q}(\tau)}|\mathcal{M}(t,\mathcal{G}(t))|+\frac{\tau}{\mathcal{Q}(\tau)\Gamma(\tau)}\int_0^t(t-\psi)^{\tau-1}|\mathcal{M}(\psi,\mathcal{G}(t))|d\psi\right\}$$

$$\leqslant \mathcal{G}(0)+\frac{1-\tau}{\mathcal{Q}(\tau)}\left[\mathfrak{K}_2\operatorname*{Sup}_{t\in K}|\mathcal{G}(t)|+\mathfrak{K}_3\right]+\frac{\tau}{\mathcal{Q}(\tau)\Gamma(q)}\int_0^t(t-\psi)^{\tau-1}\left[\mathfrak{K}_2\operatorname*{Sup}_{t\in K}|\mathcal{G}(t)|+\mathfrak{K}_3\right]d\psi$$

$$=\mathcal{G}(0)+\frac{1-\tau}{\mathcal{Q}(\tau)}\left[\mathfrak{K}_2\|\mathcal{G}(t)\|+\mathfrak{K}_3\right]+\frac{\tau}{\mathcal{Q}(\tau)\Gamma(q)}\int_0^t(t-\psi)^{\tau-1}\left[\mathfrak{K}_2\|\mathcal{G}(t)\|+\mathfrak{K}_3\right]d\psi$$

$$=\mathcal{G}(0)+\left[\frac{1-\tau}{\mathcal{Q}(\tau)}+\frac{T^\tau}{\mathcal{Q}(\tau)\Gamma(\tau)}\right]\mathfrak{K}_3+\left[\frac{1-\tau}{\mathcal{Q}(\tau)}+\frac{T^\tau}{\mathcal{Q}(\tau)\Gamma(\tau)}\right]\mathfrak{K}_2 q.$$

Thus we have

$$\|\Pi(\mathcal{G}(t))\| \leqslant \Upsilon_1+q\Upsilon_2. \tag{4.17}$$

Therefore, the operator Π maps $\mathcal{Z}_q$ into itself.

Step II: Subsequently, we demonstrate that the operator $\mathscr{U}:\mathcal{Z}_q\to\mathcal{Z}_q$ constitutes a contraction if $\frac{1-\tau}{\mathcal{Q}(\tau)}\mathfrak{K}_1<1$. Accordingly, let $\mathcal{G},\widehat{\mathcal{G}}\in\mathcal{Z}_q$ and $t\in K$ consequently, based on Theorem (4.2), we have

$$\|\mathscr{U}(\mathcal{G}(t))-\mathscr{U}(\widehat{\mathcal{G}})(t)\| = \operatorname*{Sup}_{t\in K}\left|\frac{1-\tau}{\mathcal{Q}(\tau)}\left(\mathcal{M}(t,\mathcal{G}(t))-\mathcal{M}(t,\widehat{\mathcal{G}}(t))\right)\right|$$

$$\leqslant \frac{1-\tau}{\mathcal{Q}(\tau)}\mathfrak{K}_1\operatorname*{Sup}_{t\in K}|\mathcal{G}(t)-\widehat{\mathcal{G}}(t)|$$

$$=\frac{1-\tau}{\mathcal{Q}(\tau)}\mathfrak{K}_1\|\mathcal{G}(t)-\widehat{\mathcal{G}}(t)\|.$$

It is evident that if the condition $\frac{1-\tau}{\mathcal{Q}(\tau)}\mathfrak{K}_1<1$ holds, then the operator $\mathscr{U}$ acts as a contraction mapping.

Step III: Finally, we establish that the operator $\mathscr{W}$ possesses relative compactness, which implies that it is continuous, uniformly bounded, and equi-continuous. To demonstrate the continuity of $\mathscr{W}$ as defined in equation (4.14), consider a sequence $\mathcal{G}_n\ni\lim_{n\to\infty}\mathcal{G}_n=\mathcal{G}$ in $\mathcal{Z}_q$, for $t\in K$. We obtain the following result.

$$\|\mathscr{W}(\mathcal{G}_n(t))-\mathscr{W}(\mathcal{G}(t))\| = \operatorname*{Sup}_{t\in K}\left|\frac{\tau}{\mathcal{Q}(\tau)\Gamma(\tau)}\int_0^t(t-\psi)^{\tau-1}\left[\mathcal{M}(\psi,\mathcal{G}_n(\psi))-\mathcal{M}(\psi,\mathcal{G}(\psi))\right]d\psi\right|$$

$$\leqslant \frac{\tau}{\mathcal{Q}(\tau)\Gamma(\tau)}\int_0^t(t-\psi)^{\tau-1}\operatorname*{Sup}_{t\in K}\left|\mathcal{M}(\psi,\mathcal{G}_n(\psi))-\mathcal{M}(\psi,\mathcal{G}(\psi))\right|d\psi$$

$$\leqslant \frac{T^\tau}{\mathcal{Q}(\tau)\Gamma(\tau)}\|\mathcal{M}(\psi,\mathcal{G}_n(\psi))-\mathcal{M}(\psi,\mathcal{G}(\psi))\|.$$

Therefore, given that $\mathcal{M}$ is continuous and $\mathcal{G}_n$ converges to $\mathcal{G}$, the operator $\mathscr{W}$ is also continuous. To ensure the uniform boundedness of $\mathscr{W}$ on $\mathcal{Z}_q$, let $\mathcal{G}$ be an element of $\mathcal{Z}_q$.Then, for any $t\in K$ we obtain:

$$\begin{aligned}
\|\mathscr{W}(\mathscr{G}(t))\| &= \operatorname*{Sup}_{t\in K}\left|\frac{\tau}{\mathscr{Q}(\tau)\Gamma(\tau)}\int_0^t (t-\psi)^{\tau-1}\mathcal{M}(\psi,\mathscr{G}(t))d\psi\right| \\
&\leqslant \frac{\tau}{\mathscr{Q}(\tau)\Gamma(\tau)}\int_0^t (t-\psi)^{\tau-1}\operatorname*{Sup}_{t\in K}|\mathcal{M}(\psi,\mathscr{G}(t))|d\psi \\
&= \frac{\tau}{\mathscr{Q}(\tau)\Gamma(\tau)}\int_0^t (t-\psi)^{\tau-1}\|\mathcal{M}(\psi,\mathscr{G}(t))\|d\psi \\
&\leqslant \frac{\tau}{\mathscr{Q}(\tau)\Gamma(\tau)}\int_0^t (t-\psi)^{\tau-1}[\mathfrak{K}_2\|\mathscr{G}(t)\|+\mathfrak{K}_3]d\psi \\
&\leqslant \frac{T^\tau}{\mathscr{Q}(\tau)\Gamma(\tau)}[\mathfrak{K}_2 q+\mathfrak{K}_3].
\end{aligned}$$

Thus, the operator $\mathscr{W}$ is uniformly bounded on $\mathcal{Z}_q$. Finally, to establish the equicontinuity of $\mathscr{W}$, let $\mathscr{G}$ be an element of $\mathcal{Z}_q$,and consider $t_1, t_2 \in K$ with $t_1 < t_2$. Then, we have:

$$\begin{aligned}
\|\mathscr{W}(\mathscr{G}(t_2))-\mathscr{W}(\mathscr{G}(t_1))\| &= \operatorname*{Sup}_{t\in K}\left|\frac{\tau}{\mathscr{Q}(\tau)\Gamma(\tau)}\int_0^{t_2}(t_2-\psi)^{\tau-1}\mathcal{M}(\psi,\mathscr{G}(t))d\psi\right. \\
&\quad \left.-\frac{\tau}{\mathscr{Q}(\tau)\Gamma(\tau)}\int_0^{t_1}(t_1-\psi)^{\tau-1}\mathcal{M}(\psi,\mathscr{G}(t))d\psi\right| \\
&= \operatorname*{Sup}_{t\in K}\left|\frac{\tau}{\mathscr{Q}(\tau)\Gamma(\tau)}\int_0^{t_1}(t_2-\psi)^{\tau-1}\mathcal{M}(\psi,\mathscr{G}(t))d\psi\right. \\
&\quad +\int_{t_1}^{t_2}(t_2-\psi)^{\tau-1}\mathcal{M}(\psi,\mathscr{G}(t))d\psi \\
&\quad \left.-\frac{\tau}{\mathscr{Q}(\tau)\Gamma(\tau)}\int_0^{t_1}(t_1-\psi)^{\tau-1}\mathcal{M}(\psi,\mathscr{G}(t))d\psi\right| \\
&\leqslant \frac{2(t_2-t_1)^\tau+(t_1^\tau-t_2^\tau)}{\mathscr{Q}(\tau)\Gamma(\tau)}(\mathfrak{K}_2 q+\mathfrak{K}_3).
\end{aligned}$$

The condition that $\|\mathscr{W}(\mathscr{G}(t_2))-\mathscr{W}(\mathscr{G}(t_1))\|$ approaches 0 as t_2 approaches $t_1$implies the equicontinuity of $\mathscr{W}$ on $\mathcal{Z}_q$. As a consequence, applying the Arzela-Ascoli theorem directly implies that the operator $\mathscr{W}$ is relatively compact.

As a result, applying Theorem 2.9 guarantees that the integral equation (5.7) possesses at least one solution. Due to this, this ensures that the model described by Equation (3.1) also has at least one solution. □

Theorem 4.4. *Theorem (4.2) holds with the constraint*

$$\left(\frac{1-\tau}{\mathscr{Q}(\tau)}+\frac{T^\tau}{\mathscr{Q}(\tau)\Gamma(\tau)}\right)\mathfrak{K}_1 < 1. \tag{4.18}$$

It is established that the fractional initial value problem (4.9) possesses a unique solution within the interval K.

Proof. Given (4.15), let $\mathscr{G}$ and $\widehat{\mathscr{G}}$ represent two solutions of (4.9) in $\aleph$ where t is an element of K. Subsequently

$$\begin{aligned}\|\Pi(\mathscr{G}(t)) - \Pi(\widehat{\mathscr{G}}(t))\| &\leqslant \left|\frac{1-\tau}{\mathscr{Q}(\tau)}\underset{t\in K}{Sup}\left(\mathcal{M}(t,\mathscr{G}(t)) - \mathcal{M}(t,\widehat{\mathscr{G}}(t))\right)\right| \\ &+ \left|\frac{\tau}{\mathscr{Q}(\tau)\Gamma(\tau)}\underset{t\in K}{Sup}\int_0^t (t-\psi)^{\tau-1}\left(\mathcal{M}(\psi,\mathscr{G}(\psi)) - \mathcal{M}(\psi,\widehat{\mathscr{G}}(\psi))\right)d\psi\right| \\ &\leqslant \frac{1-\tau}{\mathscr{Q}(\tau)}\mathfrak{K}_1[\mathscr{G}(t) - \widehat{\mathscr{G}}(t)] + \frac{T^\tau}{\mathscr{Q}(\tau)\Gamma(\tau)}\mathfrak{K}_1[\mathscr{G}(t) - \widehat{\mathscr{G}}(t)] \\ &\left(\frac{1-\tau}{\mathscr{Q}(\tau)} + \frac{T^\tau}{\mathscr{Q}(\tau)\Gamma(\tau)}\right)\mathfrak{K}_1[\mathscr{G}(t) - \widehat{\mathscr{G}}(t)].\end{aligned}$$

Inequality (4.18) confirms that the operator is a contraction mapping, which in turn implies that the integral Equation (5.7) has a unique solution, and consequently, the fractional model (3.1) also has a unique solution. □

5 UH stablity

The concept of Ulam-Hyers (UH) stability ensures that small perturbations in initial data or model parameters result in only small deviations in the solution, making the model robust and reliable for predicting disease dynamics. In the context of HBV modeling, UH stability is important to validate that the model's forecasts remain consistent under minor uncertainties or measurement errors.

We devote this section to examining the UH stability of the fractional model (3.1), with the aim of obtaining significant results that shed light on its stability characteristics.

Definition 5.1. We define the model (3.1), rewritten as (4.9), to be UH stable if a constant $\Delta > 0$ exists, ensuring that for all $\mathfrak{H} > 0$ and any solution $\widehat{\mathscr{G}} \in \aleph$ satisfying the inequality,

$$\|{}^{\mathscr{Q}}_0\mathfrak{D}^\tau_t\widehat{\mathscr{G}}(t) - \mathcal{M}(t,\widehat{\mathscr{G}}(t))\| \leqslant \mathfrak{H}, t \in K. \tag{5.1}$$

There exists unique solution $\mathscr{G} \in \aleph$ of (4.9) with initial condition $\mathscr{G}(0) = \widehat{\mathscr{G}}(0)$ ∋,

$$\|\widehat{\mathscr{G}}(t) - \mathscr{G}(t)\| \leqslant \Delta\mathfrak{H}, \forall t \in K, \tag{5.2}$$

where

$$\widehat{\mathscr{G}}(t) = \begin{pmatrix}\widehat{\mathcal{S}}(t)\\ \widehat{\mathcal{I}}(t)\\ \widehat{\mathcal{R}}(t)\end{pmatrix}, \quad \widehat{\mathscr{G}}(0) = \begin{pmatrix}\widehat{\mathcal{S}}(0)\\ \widehat{\mathcal{I}}(0)\\ \widehat{\mathcal{R}}(0)\end{pmatrix}, \quad \mathcal{M}(t,\widehat{\mathscr{G}}(t)) = \begin{pmatrix}\mathcal{M}_1(t,\widehat{\mathcal{S}},\widehat{\mathcal{I}},\widehat{\mathcal{R}})\\ \mathcal{M}_2(t,\widehat{\mathcal{S}},\widehat{\mathcal{I}},\widehat{\mathcal{R}})\\ \mathcal{M}_3(t,\widehat{\mathcal{S}},\widehat{\mathcal{I}},\widehat{\mathcal{R}})\end{pmatrix},$$

and

$$\mathfrak{H} = \max\begin{pmatrix}\mathfrak{H}_1\\ \mathfrak{H}_2\\ \mathfrak{H}_3\end{pmatrix}, \quad \Delta = \max\begin{pmatrix}\Delta_1\\ \Delta_2\\ \Delta_3\end{pmatrix}.$$

In the context of UH stability, the constant Δ is referred to as the stability constant for the fractional order problem (3.1).

Definition 5.2. The given problem (4.9) is considered to exhibit GUH stability if ∃ a continuous function $\mathscr{B} : K \to \mathbb{R}_+$ with $\mathscr{B}(0) = 0$, ensuring that, $\forall\ \widehat{\mathscr{G}} \in \aleph$ satisfying condition (5.1), a unique solution $\mathscr{G} \in \aleph$ of Equation (4.9) exists ∋

$$\|\widehat{\mathscr{G}}(t) - \mathscr{G}(t)\| \leqslant \mathscr{B}(\mathfrak{H}), \forall t \in \mathsf{K}. \tag{5.3}$$

Remark 5.3. To analyze the stability of the model, a small perturbation is introduced $\varpi(t) \in C(\mathsf{K})$ such that $\varpi(0) = 0$ and ensure that the following conditions are fulfilled:

(I) $|\varpi(t)| \leqslant \mathfrak{H}$ for $t \in \mathsf{K}$ and $\mathfrak{H} > 0$,

(II) ${}^{\mathscr{Q}}_{0}\mathfrak{D}^{\tau}_{t}\widehat{\mathscr{G}}(t) = \mathcal{M}(t, \widehat{\mathscr{G}}(t)) + \varpi(t)$, for all $t \in \mathsf{K}$,

where $\varpi(t) = \begin{pmatrix} \varpi_1(t) \\ \varpi_2(t) \\ \varpi_3(t) \end{pmatrix}$.

Lemma 5.4. *The solution $\widehat{\mathscr{G}_{\varpi}}(t)$ of the perturbed problem*

$$\begin{cases} {}^{\mathscr{Q}}_{0}\mathfrak{D}^{\tau}_{t}\widehat{\mathscr{G}}(t) & = \mathcal{M}(t, \widehat{\mathscr{G}}(t)) + \varpi(t), \text{ for all } t \in \mathsf{K}, \\ \widehat{\mathscr{G}}(0) & = \widehat{\mathscr{G}_0}, \end{cases} \tag{5.4}$$

fulfills the inequality

$$\|\widehat{\mathscr{G}_{\varpi}}(t) - \widehat{\mathscr{G}}(t)\| \leqslant \chi\mathfrak{H}. \tag{5.5}$$

$\widehat{\mathscr{G}}$ satisfied (5.1) and $\chi = \left(\frac{1-\tau}{\mathscr{Q}(\tau)} + \frac{T^{\tau}}{\mathscr{Q}(\tau)\Gamma(\tau)} \right)$.

Proof. From Lemma (2.7) solution of problem (5.4) is given by

$$\widehat{\mathscr{G}_{\varpi}}(t) = \widehat{\mathscr{G}_0} + \frac{1-\tau}{\mathscr{Q}(\tau)}[\mathcal{M}(t, \widehat{\mathscr{G}}(t)) + \varpi(t)] + \frac{\tau}{\mathscr{Q}(\tau)\Gamma(\tau)}\int_0^t (t-\psi)^{\tau-1}[\mathcal{M}(\psi, \widehat{\mathscr{G}}(\psi)) + \varpi(\psi)]d\psi. \tag{5.6}$$

Additionally, we possess

$$\widehat{\mathscr{G}}(t) = \widehat{\mathscr{G}_0} + \frac{1-\tau}{\mathscr{Q}(\tau)}[\mathcal{M}(t, \widehat{\mathscr{G}}(t))] + \frac{\tau}{\mathscr{Q}(\tau)\Gamma(\tau)}\int_0^t (t-\psi)^{\tau-1}[\mathcal{M}(\psi, \widehat{\mathscr{G}}(\psi))]d\psi. \tag{5.7}$$

Remark 5.3 leads to the conclusion that

$$\begin{aligned} \|\widehat{\mathscr{G}_{\varpi}}(t) - \widehat{\mathscr{G}}(t)\| &\leqslant \frac{1-\tau}{\mathscr{Q}(\tau)}\|\varpi(t)\| + \frac{\tau}{\mathscr{Q}(\tau)\Gamma(\tau)}\int_0^t (t-\psi)^{\tau-1}\|\varpi(\psi)\|d\psi \\ &\leqslant \left(\frac{1-\tau}{\mathscr{Q}(\tau)} + \frac{T^{\tau}}{\mathscr{Q}(\tau)} \right)\mathfrak{H}. \end{aligned} \tag{5.8}$$

This implies

$$\|\widehat{\mathscr{G}_{\varpi}}(t) - \widehat{\mathscr{G}}(t)\| \leqslant \chi\mathfrak{H}. \tag{5.9}$$

□

Theorem 5.5. Under the conditions stated in Lemma 5.4, the solution to the fractional initial value problem (IVP) exhibits both UH stability and GUH stability in $\aleph$ provided that $(1 - \aleph_1\chi) > 0$.

Therefore, the fractional model (3.1) is demonstrated to be UH stable as well as satisfying GUH stability in $\aleph$.

Proof. Let $\widehat{\mathscr{G}} \in \aleph$ fulfill the inequality (5.1), and let $\widehat{\mathscr{G}}$ be the unique solution to the problem (4.9) with the starting condition $\mathscr{G}(0) = \widehat{\mathscr{G}}(0) \Longleftrightarrow \mathscr{G}_0 = \widehat{\mathscr{G}_0}$. Consequently, it concludes from Lemma 2.7 that

$$\mathscr{G} = \widehat{\mathscr{G}_0} + \frac{1-\tau}{\mathscr{Q}(\tau)}\mathcal{M}(t,\mathscr{G}(t)) + \frac{\tau}{\mathscr{Q}(\tau)\Gamma(\tau)}\int_0^t (t-\psi)^{\tau-1}\mathcal{M}(\psi,\mathscr{G}(\psi))d\psi, \tag{5.10}$$

$$\begin{aligned}
\|\widehat{\mathscr{G}}(t) - \mathscr{G}(t)\| &= \left\| \widehat{\mathscr{G}}(t) - \left(\widehat{\mathscr{G}_0} + \frac{1-\tau}{\mathscr{Q}(\tau)}\mathcal{M}(t,\mathscr{G}(t)) + \frac{\tau}{\mathscr{Q}(\tau)\Gamma(\tau)}\int_0^t (t-\psi)^{\tau-1}\mathcal{M}(\psi,\mathscr{G}(\psi))d\psi \right) \right\| \\
&= \left\| \widehat{\mathscr{G}}(t) - \left(\widehat{\mathscr{G}_0} + \frac{1-\tau}{\mathscr{Q}(\tau)}\mathcal{M}(t,\mathscr{G}(t)) + \frac{\tau}{\mathscr{Q}(\tau)\Gamma(\tau)}\int_0^t (t-\psi)^{\tau-1}\mathcal{M}(\psi,\mathscr{G}(\psi))d\psi \right) \right. \\
&\quad + \left(\widehat{\mathscr{G}_0} + \frac{1-\tau}{\mathscr{Q}(\tau)}[\mathcal{M}(t,\widehat{\mathscr{G}}(t)) + \varpi(t)] + \frac{\tau}{\mathscr{Q}(\tau)\Gamma(\tau)}\int_0^t (t-\psi)^{\tau-1}[\mathcal{M}(\psi,\widehat{\mathscr{G}}(\psi)) \right. \\
&\quad \left. + \varpi(\psi)]d\psi \right) - \left(\widehat{\mathscr{G}_0} + \frac{1-\tau}{\mathscr{Q}(\tau)}[\mathcal{M}(t,\widehat{\mathscr{G}}(t)) + \varpi(t)] + \frac{\tau}{\mathscr{Q}(\tau)\Gamma(\tau)}\int_0^t (t-\psi)^{\tau-1} \right. \\
&\quad \left. \left. [\mathcal{M}(\psi,\widehat{\mathscr{G}}(\psi)) + \varpi(\psi)]d\psi \right) \right\| \\
&\leqslant 2\chi\mathfrak{H} + \frac{1-\tau}{\mathscr{Q}(\tau)}\mathfrak{K}_1\|[\mathscr{G}(t) - \widehat{\mathscr{G}}(t)]\| + \frac{T^\tau}{\mathscr{Q}(\tau)\Gamma(\tau)}\mathfrak{K}_1\|[\mathscr{G}(t) - \widehat{\mathscr{G}}(t)]\| \\
&\leqslant 2\chi\mathfrak{H} + \left(\frac{1-\tau}{\mathscr{Q}(\tau)} + \frac{T^\tau}{\mathscr{Q}(\tau)\Gamma(\tau)} \right)\mathfrak{K}_1\|[\mathscr{G}(t) - \widehat{\mathscr{G}}(t)]\|.
\end{aligned} \tag{5.11}$$

$\Rightarrow$

$$\|\widehat{\mathscr{G}}(t) - \mathscr{G}(t)\| \leqslant \frac{2\chi\mathfrak{H}}{1-\mathfrak{K}_1\chi}. \tag{5.12}$$

For $\Delta = \frac{2\chi\mathfrak{H}}{1-\mathfrak{K}_1\chi}$ with $1 - \mathfrak{K}_1\chi > 0$, the inequality in (5.12) suggests

$$\|\widehat{\mathscr{G}}(t) - \mathscr{G}(t)\| \leqslant \Delta\mathfrak{H}. \tag{5.13}$$

As a result, the fractional IVP (4.9) solution is UH stable. Furthermore, by defining $\mathscr{B}(\mathfrak{H}) = \Delta\mathfrak{H}$ with $\mathscr{B}(0) = 0$ in a way that satisfies

$$\|\widehat{\mathscr{G}}(t) - \mathscr{G}(t)\| \leqslant \mathscr{B}(\mathfrak{H}). \tag{5.14}$$

The analysis confirms that the fractional IVP (4.9) meets the criteria for GUH stability. Thus, the proposed model (3.1) possesses both UH and GUH stability.

□

6 Equilibrium point, their stability, and basic reproduction number

This section calculates the basic reproduction number to evaluate the transmission of infection in the suggested model. In an epidemic model, equilibrium points represent constant values of the variables that remain unchanged over time, indicating a stable state in which the prevalence of the disease remains steady. In an epidemic model, two significant steady states are the Hepatitis B-free equilibrium (HBFE) and Hepatitis B-present equilibrium point (HBPE).

6.1 Hepatitis B-free equilibrium (HBFE) point

To identify the equilibrium points of the fractionalized Hepatitis B model (3.1), we proceed by introducing

$$\begin{cases} \theta - (1-\zeta)\frac{\beta \widehat{\mathcal{S}}_* \widehat{\mathcal{I}}_*}{1+k_1\widehat{\mathcal{S}}_*+k_2\widehat{\mathcal{I}}_*} - (\mu+m)\widehat{\mathcal{S}}_* = 0, \\ (1-\zeta)\frac{\beta \widehat{\mathcal{S}}_* \widehat{\mathcal{I}}_*}{1+k_1\widehat{\mathcal{S}}_*+k_2\widehat{\mathcal{I}}_*} - (\mu+\delta+\eta)\widehat{\mathcal{I}}_* = 0, \\ \eta\widehat{\mathcal{I}}_* + m\widehat{\mathcal{S}}_* - \mu\widehat{\mathcal{R}}_* = 0. \end{cases} \tag{6.1}$$

HBFE point of model (3.1) represents the steady state in which Hepatitis B is absent from the studied population. We take $\widehat{\mathcal{I}}_* = 0$. Then we get HBFE point is

$$\widehat{\mathcal{H}}_* = (\widehat{\mathcal{S}}_*, \widehat{\mathcal{I}}_*, \widehat{\mathcal{R}}_*) = \left(\frac{\theta}{\mu+m}, 0, \frac{\theta m}{(\mu+m)\mu}\right).$$

6.2 The basic reproduction number

The basic reproduction number is a key factor in public health decision-making, as it guides interventions aimed at controlling the spread of infections.We employ the next-generation matrix (NGM) [53] approach to calculate the basic reproduction number for our system, denoted as $\mathscr{R}_0$. In this approach, we identify $\mathfrak{F}_i$ and $\mathscr{V}_i$ from the infected compartments of the model, where $\mathfrak{F}_i$ represents the progression into the infected classes, and $\mathscr{V}_i$ signifies the removal from the infected classes.
$\mathfrak{F}_i$ and $\mathscr{V}_i$ define as follows:

$$\mathfrak{F}_i = \left((1-\zeta)\frac{\beta\widehat{\mathcal{S}}\widehat{\mathcal{I}}}{1+k_1\widehat{\mathcal{S}}+k_2\widehat{\mathcal{I}}}\right) \text{ and } \mathscr{V}_i = \left((\mu+\delta+\eta)\widehat{\mathcal{I}}\right).$$

The Jacobian matrix of $\mathfrak{F}_i$ and $\mathscr{V}_i$ at $\widehat{\mathcal{H}}_*$ given as :

$$\mathcal{F}\big|_{\widehat{\mathcal{H}}_*} = \left(\frac{(1-\zeta)\widehat{\mathcal{S}}_*\beta(k_1\widehat{\mathcal{S}}_*+1)}{(1+k_1\widehat{\mathcal{S}}_*+k_2\widehat{\mathcal{I}}_*)^2}\right).$$

$$\mathcal{V}\big|_{\widehat{\mathcal{H}}_*} = \left(\mu+\delta+\eta\right).$$

$\mathscr{R}_0$ is spectral radisus of matrix $\mathcal{F}\mathcal{V}^{-1}\big|_{\widehat{\mathcal{H}}_*}$ is given by :

$$\mathscr{R}_0 = \frac{(1-\zeta)\theta\beta}{(\theta k_1 + m + \mu)(\mu+\delta+\eta)}.$$

6.3 Local stablity analysis (LAS)

Theorem 6.1. *If $\mathscr{R}_0 < 1$ then HBFE $\mathscr{P}^0$ of the proposed Hepatitis B model (3.1) is LAS, otherwise, it becomes unstable.*

Proof. To demonstrate the desired result, we calculate the Jacobian matrix of the proposed Hepatitis B model system (3.1) at $\widehat{\mathcal{H}}_*$

$$\mathfrak{J}\big|_{\widehat{\mathcal{H}}_*} = \begin{pmatrix} -(\mu+m) & -\frac{(1-\zeta)\beta\theta}{(\mu+m+\theta k_1)} & 0 \\ 0 & (\mu+\delta+\eta)(\mathscr{R}_0-1) & 0 \\ m & \eta & -\mu \end{pmatrix}.$$

Eigen values of the matrix $\mathfrak{J}\big|_{\widehat{\mathcal{H}}_*}$ is given by :

$$\begin{aligned}\widehat{\lambda}_1 &= -(\mu + m),\\ \widehat{\lambda}_2 &= -(\mu),\\ \widehat{\lambda}_3 &= (\mu + \delta + \eta)(\mathscr{R}_0 - 1).\end{aligned}$$

We observe that for $\gamma \in (0,1], |arg(\widehat{\lambda}_1)| = \pi > \frac{\gamma\pi}{2}$, $|arg(\widehat{\lambda}_2)| = \pi > \frac{\gamma\pi}{2}$, and $|arg(\widehat{\lambda}_3)| = \pi > \frac{\gamma\pi}{2}$ if $\mathscr{R}_0 < 1$. Hence, the HBFE $\widehat{\mathcal{H}}_*$ of the system is LAS if $\mathscr{R}_0 < 1$. □

6.4 Hepatitis B present equilibrium (HBPE) point

To identify the HBPE points, the system of differential equations in model (3.1) is set to zero. Solving the resulting equations provides the HBPE. $\widehat{\mathcal{H}}_{**} = \left(\widehat{\mathcal{S}}_{**}, \widehat{\mathcal{I}}_{**}, \widehat{\mathcal{R}}_{**}\right)$

$$\begin{cases}\widehat{\mathcal{S}}_{**} = \frac{(\theta k_2+\eta+m+\mu)\theta}{(\mu+\delta+\eta)((\mathscr{R}_0-1)(m+\mu)+k_1\theta\mathscr{R}_0)+k_2\theta(m+\mu)},\\ \widehat{\mathcal{I}}_{**} = \frac{(\mathscr{R}_0-1)\theta(\theta k_1+m+\mu)}{(\mu+\delta+\eta)((\mathscr{R}_0-1)(m+\mu)+k_1\theta\mathscr{R}_0)+k_2\theta(m+\mu)},\\ \widehat{\mathcal{R}}_{**} = \frac{1}{(\mu+\delta+\eta)((\mathscr{R}_0-1)(m+\mu)+k_1\theta\mathscr{R}_0)+k_2\theta(m+\mu)}\left[\frac{m}{\mu}(\theta k_2+\eta+m+\mu)\theta + \frac{\eta}{\mu}(\mathscr{R}_0-1)\theta(\theta k_1+m+\mu)\right].\end{cases} \tag{6.2}$$

Theorem 6.2. *HBPE $\widehat{\mathcal{H}}_{**}$ of the model (3.1) is LAS if $\mathscr{R}_0 > 1$.*

Proof. We consider the Jacobian matrix of the system (3.1) evaluated at the HBPE point $\widehat{\mathcal{H}}_{**} = (\widehat{\mathcal{S}}_{**}, \widehat{\mathcal{I}}_{**}, \widehat{\mathcal{R}}_{**})$.

$$\mathfrak{J}\big|_{\widehat{\mathcal{H}}_{**}} = \begin{pmatrix}\widehat{\mathfrak{d}}_{11} & \widehat{\mathfrak{d}}_{12} & \widehat{\mathfrak{d}}_{13}\\ \widehat{\mathfrak{d}}_{21} & \widehat{\mathfrak{d}}_{22} & \widehat{\mathfrak{d}}_{23}\\ \widehat{\mathfrak{d}}_{31} & \widehat{\mathfrak{d}}_{32} & \widehat{\mathfrak{d}}_{33}\end{pmatrix},$$

where

$$\begin{cases}\widehat{\mathfrak{d}}_{11} = -\frac{\left(\theta(1-\zeta)\beta-(\mu+\delta+\eta)(m+\mu+k_1\theta)((1-\zeta)\beta-k_1(\mu+\delta+\eta))\right)}{\beta(1-\zeta)(1-p)^{\alpha}(\mu+\delta+\eta+k_2\theta)} - (m+\mu),\\ \widehat{\mathfrak{d}}_{12} = -\frac{(\mu+\delta+\eta)^2\left(\beta(1-\zeta)+k_2(\mu+m+k_1\theta)\right)}{\beta(1-\zeta)(\mu+\delta+\eta+k_2\theta)},\\ \widehat{\mathfrak{d}}_{13} = 0,\\ \widehat{\mathfrak{d}}_{21} = \frac{\left(\theta(1-\zeta)\beta-(\mu+\delta+\eta)(m+\mu+k_1\theta)((1-\zeta)\beta-k_1(\mu+\delta+\eta))\right)}{\beta(1-\zeta)(\mu+\delta+\eta+k_2\theta)},\\ \widehat{\mathfrak{d}}_{22} = \frac{(\mu+\delta+\eta)^2\left(\beta(1-\zeta)+k_2(\mu+m+k_1\theta)\right)}{\beta(1-\zeta)(\mu+\delta+\eta+k_2\theta)} - (\mu+\delta+\eta),\\ \widehat{\mathfrak{d}}_{23} = 0,\\ \widehat{\mathfrak{d}}_{31} = m,\\ \widehat{\mathfrak{d}}_{32} = \eta,\\ \widehat{\mathfrak{d}}_{33} = -\mu.\end{cases}$$

Eigen value of the matrix $\mathfrak{J}\big|_{\widehat{\mathcal{H}}_{**}}$ is given by :

$\widehat{d}_1 = -\mu$, remaining eigen values of $\mathfrak{J}\big|_{\widehat{\mathcal{H}}_{**}}$ is eigen values of the following matrix $\mathfrak{P}\big|_{\widehat{\mathcal{H}}_{**}} = \begin{pmatrix} \widehat{\eth}_{11} & \widehat{\eth}_{12} \\ \widehat{\eth}_{21} & \widehat{\eth}_{22} \end{pmatrix}$. Trace and determinant of the matrix $\mathfrak{P}\big|_{\widehat{\mathcal{H}}_{**}}$ as follows:

$$\mathrm{Tr}(\mathfrak{P}\big|_{\widehat{\mathcal{H}}_{**}}) = -\frac{(\mathscr{R}_0-1)(\mu+\delta+\eta)^2(m+\mu+k_1\theta)[\mathscr{R}_0(\mu+m)+(\mathscr{R}_0-1)k_1\theta+k_2\theta]}{\beta(1-\zeta)\theta(\mu+\delta+\eta+k_2\theta)} - (m+\mu),$$

$$\det(\mathfrak{P}\big|_{\widehat{\mathcal{H}}_{**}}) = \frac{\begin{pmatrix}(\mathscr{R}_0-1)(\mu+\delta+\eta)^2(m+\mu+k_1\theta)[\mathscr{R}_0(\mu+m)(\mu+\delta+\eta)\\ +(\mathscr{R}_0-1)k_1\theta(\mu+\delta+\eta)+k_2(\mu+m)]\end{pmatrix}}{\beta(1-\zeta)\theta(\mu+\delta+\eta+k_2(\theta))}.$$

It is easily seen that $\mathrm{Tr}(\mathfrak{P}\big|_{\widehat{\mathcal{H}}_{**}}) < 0$ and $\det(\mathfrak{P}\big|_{\widehat{\mathcal{H}}_{**}}) > 0$. Then eigen values of Jacobian matrix $\mathfrak{J}\big|_{\widehat{\mathcal{H}}_{**}}$ such that $|\arg(\widehat{d}_j)| > \frac{\gamma\pi}{2}$, $\forall\, j = 1,2,3$ and $\gamma \in (0,1]$, HBPE $\widehat{\mathcal{H}}_{**}$ is LAS.

□

6.5 Global asymptotic stability (GAS) of HBPE point

The global stability of HBPE is crucial for understanding the long-term behavior of Hepatitis transmission. It ensures that the system stabilizes at a steady state regardless of initial conditions. We state and prove the following theorem for the GAS of the HBPE using the Lyapunov function method, demonstrating that all trajectories of the system converge to the endemic equilibrium. This study offers significant insights into illness persistence and management techniques.

Theorem 6.3. *The HBPE point $\widehat{\mathcal{H}}_{**}$ is GAS whenever $\mathfrak{R}_0 > 1$.*

Proof. To establish the theorem, we define the as follows:

$$\mathfrak{L} = \frac{1}{2}\big[(\widehat{\mathcal{S}}-\widehat{\mathcal{S}}_{**}) + (\widehat{\mathcal{I}}-\widehat{\mathcal{I}}_{**}) + (\widehat{\mathcal{R}}-\widehat{\mathcal{R}}_{**})\big]^2. \tag{6.3}$$

From the Lemma 2.8 we obtain

$${}_0^{\mathscr{Z}}\mathfrak{D}_t^{\tau}\mathfrak{L}(t) \leqslant -\mu\big[(\widehat{\mathcal{S}}-\widehat{\mathcal{S}}_{**}) + (\widehat{\mathcal{I}}-\widehat{\mathcal{I}}_{**}) + (\widehat{\mathcal{R}}-\widehat{\mathcal{R}}_{**})\big]\big[\widehat{\mathcal{S}}+\widehat{\mathcal{I}}+\widehat{\mathcal{R}}-\tfrac{\theta}{\mu}\big],$$

$${}_0^{\mathscr{Z}}\mathfrak{D}_t^{\tau}\mathfrak{L}(t) \leqslant -\mu\big[(\widehat{\mathcal{S}}-\widehat{\mathcal{S}}_{**}) + (\widehat{\mathcal{I}}-\widehat{\mathcal{I}}_{**}) + (\widehat{\mathcal{R}}-\widehat{\mathcal{R}}_{**})\big]\big[(\widehat{\mathcal{S}}-\widehat{\mathcal{S}}_{**}) + (\widehat{\mathcal{I}}-\widehat{\mathcal{I}}_{**}) + (\widehat{\mathcal{R}}-\widehat{\mathcal{R}}_{**})\big],$$

$${}_0^{\mathscr{Z}}\mathfrak{D}_t^{\tau}\mathfrak{L}(t) \leqslant -\big[(\widehat{\mathcal{S}}-\widehat{\mathcal{S}}_{**}) + (\widehat{\mathcal{I}}-\widehat{\mathcal{I}}_{**}) + (\widehat{\mathcal{R}}-\widehat{\mathcal{R}}_{**})\big]^2.$$

Thus ${}_0^{\mathscr{Z}}\mathfrak{D}_t^{\tau}\mathfrak{L}(t) \leqslant 0, \forall\, (\widehat{\mathcal{S}},\widehat{\mathcal{I}},\widehat{\mathcal{R}}) \in \widehat{\mho}$. Thus $\mathfrak{L}$ is bounded, non-increasing, continuous, and differentiable function. Moreover, ${}_0^{\mathscr{Z}}\mathfrak{D}_t^{\tau}\mathfrak{L}(t) = 0$ iff $\widehat{\mathcal{S}} = \widehat{\mathcal{S}}_{**}$, $\widehat{\mathcal{I}} = \widehat{\mathcal{I}}_{**}$, $\widehat{\mathcal{R}} = \widehat{\mathcal{R}}_{**}$.Therefore, we can say that $\mathfrak{L}$ is a positive-definite function. the HBPE point of proposed model (3.1) is GAS when $\mathfrak{R}_0 > 1$. This concludes the proof of Theorem (6.3). □

7 Sensitivity

Conducting sensitivity analysis is crucial for understanding how various parameters influence disease transmission. It helps in understanding how changes in specific parameters affect the reproduction number, providing insights into key factors that drive disease dynamics. Identifying these critical parameters enables the formulation of effective intervention strategies to mitigate

disease spread. The sensitivity index of a function $\wp(y_1, y_2, \cdots, y_n)$ with respect to a parameter $y_i, (i = 1, 2, \cdots, n)$ is denoted as $\Xi^{\wp}_{y_i}$ and is defined as

$$\Xi^{\wp}_{y_i} = \frac{\partial \wp}{\partial y_i} \times \frac{y_i}{\wp}, \tag{7.1}$$

$$\begin{cases} \Xi^{\mathscr{R}_0}_{\zeta} &= -\frac{\zeta}{1-\zeta}, \\ \Xi^{\mathscr{R}_0}_{\beta} &= 1, \\ \Xi^{\mathscr{R}_0}_{\theta} &= \frac{m+\mu}{\theta k_1+m+\mu}, \\ \Xi^{\mathscr{R}_0}_{k_1} &= -\frac{k_1\theta}{\theta k_1+m+\mu}, \end{cases} \quad \begin{cases} \Xi^{\mathscr{R}_0}_{m} &= -\frac{m}{\theta k_1+m+\mu}, \\ \Xi^{\mathscr{R}_0}_{\mu} &= -\frac{(\theta k_1+\delta+\eta+m+2\mu)\mu}{(\mu+\delta+\eta)(\theta k_1+m+\mu)}, \\ \Xi^{\mathscr{R}_0}_{\delta} &= -\frac{\delta}{\mu+\delta+\eta}, \\ \Xi^{\mathscr{R}_0}_{\eta} &= -\frac{\eta}{\mu+\delta+\eta}. \end{cases}$$

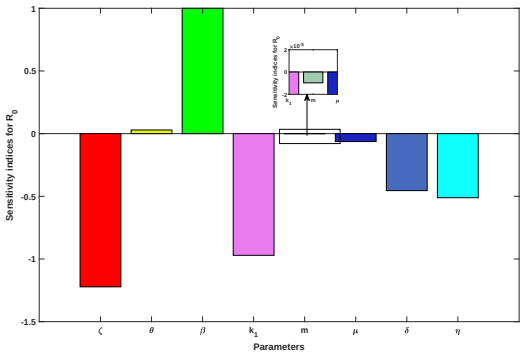

Figure 1: Sensitivity analysis of factors influencing $\mathscr{R}_0$.

Figure (1) illustrates the sensitivity analysis of the basic reproduction number $\mathscr{R}_0$ with respect to key model parameters. It is evident from the figure that the parameters θ and β are positively correlated with the reproduction number. This positive correlation implies that an increase in either θ or β leads to a proportional rise in $\mathscr{R}_0$ thereby enhancing the potential for disease transmission. On the other hand, parameters such as ζ, k_1, m, μ, δ, and η are shown to have a negative correlation with the reproduction number. This indicates that increases in these parameters contribute to a decrease in $\mathscr{R}_0$,thus reducing the potential for the spread of infection. Overall, the sensitivity analysis highlights the critical role of targeted control measures. Interventions that reduce the values of positively correlated parameters or increase the values of negatively correlated ones can effectively suppress the reproduction number below unity, which is essential for disease eradication.

8 Model fitting and parameter estimation

This section validates the model using reported Hepatitis B data from 2011 to 2018 in United States, [54]. Figure 2(a) displays the fitting of the Hepatitis B model. Figure 2(b) shows a random distribution of residuals, indicating a well-fitted model. The parameters to be estimated is σ. The other parameters are obtained from the literature and given in Table 2. The estimated values of $\beta = 0.3611$

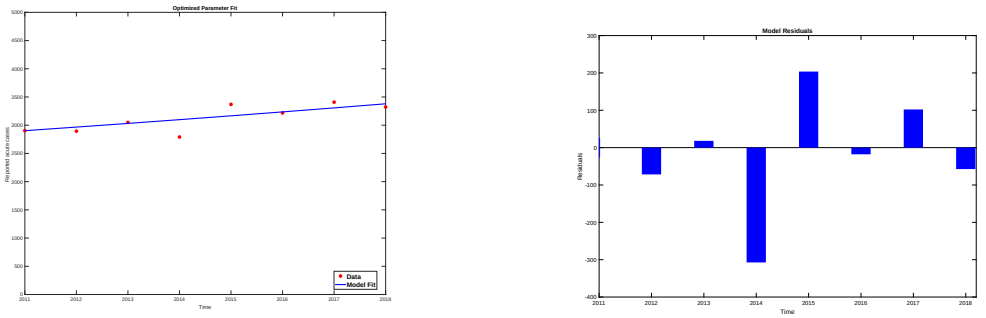

(a) (b)

Figure 2: Model fitting and residuals

9 Numerical scheme

An iterative method is introduced here to demonstrate the dynamic behavior of Hepatitis B infection. This approach builds on the methodology outlined in [55] for fractional models and is detailed as follows:

$$ {}^{\mathscr{Q}}_{0}\mathfrak{D}^{\tau}_{t}\mathscr{G}(t) = \mathcal{M}(t,\mathscr{G}(t)). \tag{9.1} $$

The fractional differential Equation (9.1) can be reformulated as a fractional integral equation. Utilizing the fundamental theorem of fractional calculus, we obtain the subsequent result.

$$ \mathscr{G}(t) - \mathscr{G}(0) = \frac{1-\tau}{\mathscr{Q}(\tau)}\mathcal{M}(t,\mathscr{G}(t)) + \frac{\tau}{\mathscr{Q}(\tau)\Gamma(\tau)}\int_0^t (t-\psi)^{\tau-1}\mathcal{F}(\psi,\mathscr{G}(\psi))\mathrm{d}p\psi, \tag{9.2} $$

where $\mathscr{Q}(\tau) = 1-\tau+\frac{\tau}{\Gamma(\tau)}$ is normalization function Equation (9.2) can be rewritten as

$$ \begin{aligned} \mathscr{G}(t_{j+1}) - \mathscr{G}(0) &= \frac{\Gamma(\tau)(1-\tau)}{\Gamma(\tau)(1-\tau)+\tau}\mathcal{M}(t_j,\mathscr{G}(t_j)) \\ &+ \frac{\tau}{\Gamma(\tau)+\tau(1-\Gamma(\tau))}\sum_{k=0}^{j}\int_{t_k}^{t_{k+1}} \mathcal{M}(\psi,\mathscr{G}(\psi)(t_{k+1}-\psi)^{\psi-1}\mathrm{d}\psi. \end{aligned} \tag{9.3} $$

The two-step Lagrange polynomial interpolation yields an approximation value for the function $\mathcal{M}(\psi,\mathscr{G}(\psi))$ in the interval $[t_k, t_{k+1}]$

$$ \beth(\Psi) \simeq \frac{\mathcal{M}(t_k,\mathscr{G}_k)}{h}(\psi - t_{k-1}) - \frac{\mathcal{M}(t_{k-1},\mathscr{G}_{k-1})}{h}(\psi - t_k). \tag{9.4} $$

By inserting Equation (9.4) into Equation (9.3), we derive the subsequent expression.

$$ \left.\begin{aligned} \mathscr{G}_{j+1}(t) = \mathscr{G}_0 + \tfrac{(1-\tau)\Gamma(\tau)}{\tau+(1-\tau)\Gamma(\tau)}\mathcal{M}(t_j,\mathscr{G}(t_j)) + \tfrac{\tau}{\Gamma(\tau)+\tau(1-\Gamma(\tau))} \\ +\sum_{k=0}^{j}\left(\frac{\mathcal{M}(t_k,\mathscr{G}_k)}{h}\int_{t_k}^{t_{k+1}}(\Psi - t_{k-1})(t_{j+1}-\psi)^{\tau-1}\mathrm{d}\psi - \right. \\ \left. \tfrac{\mathcal{M}(t_{k-1},\mathscr{G}_{k-1})}{h}\int_{t_k}^{t_{k+1}}(\psi - t_k)(t_{j+1}-\psi)^{\tau-1}\mathrm{d}\psi\right). \end{aligned}\right\} \tag{9.5} $$

For simplicity, we let

$$\left.\begin{aligned}\mathfrak{B}_{\tau,k,1} &= \int_{t_k}^{t_{k+1}} (\psi - t_{k-1})(t_{j+1} - \psi)^{\tau-1} d\psi,\\ \mathfrak{B}_{\tau,k,2} &= \int_{t_k}^{t_{k+1}} (\psi - t_k)(t_{j+1} - \Psi)^{\tau-1} d\psi.\end{aligned}\right\} \tag{9.6}$$

which implies that

$$\left.\begin{aligned}\mathfrak{B}_{\xi,k,1} &= h^{\xi+1} \tfrac{(j+1-k)^{\xi}(j-k+2+\xi)-(j-k)^{\xi}(j-k+2-2\xi)}{\xi(\xi+1)},\\ \mathfrak{B}_{\xi,k,2} &= h^{\xi+1} \tfrac{(j+1-k)^{j+1}-(j-k)^{\xi}(j-k+1+\xi)}{\xi(\xi+1)}.\end{aligned}\right\} \tag{9.7}$$

When substituted integration (9.7) into Eq. (9.5), provides a viable approximation.

$$\left.\begin{aligned}\mathscr{G}_{j+1}(t) = \mathscr{G}_0 + \tfrac{(1-\tau)\Gamma(\tau)}{\tau+(1-\tau)\Gamma(\tau)}\mathcal{M}(t_j, \mathscr{G}(t_j)) + \tfrac{1}{\tau+(1+\tau)(1-\tau)\Gamma(\tau)}\\ \times\sum_{k=0}^{j}\Big(h^{\tau}\mathcal{M}(t_k,\mathscr{G}_k)\big((j+1-k)^{\tau}(j-k+2+\tau)-\\ (j-k)^{\tau}(j-k+2+2\tau)\big) - h^{\tau}\mathcal{M}(t_{k-1},\mathscr{G}_{k-1})\big((j+1-k)^{\tau+1}\\ -(j-k)^{\tau}\times(j-k+1+\tau)\big)\Big).\end{aligned}\right\} \tag{9.8}$$

Lastly, the numerical solution of the model (3.1) is determined as follows.

$$\left.\begin{aligned}\widehat{\mathcal{S}}_{j+1}(t) = \widehat{\mathcal{S}}_0 + \tfrac{(1-\tau)\Gamma(\tau)}{\tau+(1-\tau)\Gamma(\tau)}\mathcal{M}_1(t_j,\widehat{\mathcal{S}}(t_j),\widehat{\mathcal{I}}(t_j),\widehat{\mathcal{R}}(t_j)) + \tfrac{1}{\tau+(1+\tau)(1-\tau)\Gamma(\tau)}\\ \times\sum_{k=0}^{j}\Big(h^{\tau}\mathcal{M}_1(t_k,\widehat{\mathcal{S}}_k,\widehat{\mathcal{I}}_k,\widehat{\mathcal{R}}_k)\big((j+1-k)^{\tau}(j-k+2+\tau)-\\ (j-k)^{\tau}(j-k+2+2\tau)\big) - h^{\tau}\mathcal{M}_1(t_{k-1},\widehat{\mathcal{S}}_{k-1},\widehat{\mathcal{I}}_{k-1},\widehat{\mathcal{R}}_{k-1})\big((j+1-k)^{\tau+1}\\ -(j-k)^{\tau}\times(j-k+1+\tau)\big)\Big).\end{aligned}\right\} \tag{9.9}$$

$$\left.\begin{aligned}\widehat{\mathcal{I}}_{j+1}(t) = \widehat{\mathcal{I}}_0 + \tfrac{(1-\tau)\Gamma(\tau)}{\tau+(1-\tau)\Gamma(\tau)}\mathcal{M}_2(t_j,\widehat{\mathcal{S}}(t_j),\widehat{\mathcal{I}}(t_j),\widehat{\mathcal{R}}(t_j)) + \tfrac{1}{\tau+(1+\tau)(1-\tau)\Gamma(\tau)}\\ \times\sum_{k=0}^{j}\Big(h^{\tau}\mathcal{M}_2(t_k,\widehat{\mathcal{S}}_k,\widehat{\mathcal{I}}_k,\widehat{\mathcal{R}}_k)\big((j+1-k)^{\tau}(j-k+2+\tau)-\\ (j-k)^{\tau}(j-k+2+2\tau)\big) - h^{\tau}\mathcal{M}_2(t_{k-1},\widehat{\mathcal{S}}_{k-1},\widehat{\mathcal{I}}_{k-1},\widehat{\mathcal{R}}_{k-1})\big((j+1-k)^{\tau+1}\\ -(j-k)^{\tau}\times(j-k+1+\tau)\big)\Big).\end{aligned}\right\} \tag{9.10}$$

$$\left.\begin{aligned}\widehat{\mathcal{R}}_{j+1}(t) = \widehat{\mathcal{R}}_0 + \tfrac{(1-\tau)\Gamma(\tau)}{\tau+(1-\tau)\Gamma(\tau)}\mathcal{M}_3(t_j,\widehat{\mathcal{S}}(t_j),\widehat{\mathcal{I}}(t_j),\widehat{\mathcal{R}}(t_j)) + \tfrac{1}{\tau+(1+\tau)(1-\tau)\Gamma(\tau)}\\ \times\sum_{k=0}^{j}\Big(h^\tau\mathcal{M}_3(t_k,\widehat{\mathcal{S}}_k,\widehat{\mathcal{I}}_k,\widehat{\mathcal{R}}_k)\big((j+1-k)^\tau(j-k+2+\tau)-\\ (j-k)^\tau(j-k+2+2\tau)\big) - h^\tau\mathcal{M}_3(t_{k-1},\widehat{\mathcal{S}}_{k-1},\widehat{\mathcal{I}}_{k-1},\widehat{\mathcal{R}}_{k-1})\big((j+1-k)^{\tau+1}\\ -(j-k)^\tau\times(j-k+1+\tau)\big)\Big).\end{aligned}\right\} \tag{9.11}$$

The numerical simulations were carried out using the parameter values listed in Table 2. The transmission rate β was estimated from real data [54], while the remaining parameters were obtained from a literature survey, as cited in the table.

Table 2: Parameters of the model and their corresponding values.

Parameter	Value	Source	Parameter	Value	Source
θ	100	Assumed	k_2	0.6	[56]
ζ	0.55	Estimated from [57]	μ	0.06	[56]
β	0.3611	Estimated	m	0.00002	[56]
k_1	0.02	Assumed	δ	0.8	Estimated from [56]
η	0.9	[56]			

9.1 Numerical simulation

We formulated an Atangana-Baleanu fractional-order mathematical model for Hepatitis B that integrates awareness and a Beddington-DeAngelis-type incidence rate. This model accounts for preventive measures adopted by susceptible individuals and the suppressive effects of treatment on infected individuals. Figure 3 illustrates the dynamic interactions among susceptible, infected, and recovered populations under different fractional orders, specifically $\tau = 0.83, 0.88, 0.93,$ and 0.98. The results indicate that as the fractional order increases, the populations of all three groups also rise. This trend highlights the substantial impact of memory effects on disease progression and recovery. To assess the influence of the contact rate (β) on disease dynamics, we varied its value as $\beta = 0.3,\ 0.5,\ 0.7,$ and 0.9. Figure 4 presents the results, demonstrating notable changes in population distribution. Specifically, Figure 4(a) shows that a higher contact rate leads to a decline in the susceptible population, indicating increased disease transmission. In contrast, Figure 4(b) depicts a rise in the infected population, signifying enhanced spread of the infection. Moreover, Figure 4(c) illustrates an increase in the recovered population, suggesting that more individuals contract and eventually recover from the disease. These findings emphasize the crucial role of the contact rate in shaping Hepatitis B transmission patterns within the model. As the awareness rate (ζ) increases, with values $\zeta = 0.22, 0.33, 0.44,$ and 0.55, Figure 5(a) depicts a rise in the susceptible population, reflecting a reduction in transmission. Concurrently, Figure 5(b) shows a decrease in the infected population, demonstrating the effectiveness of awareness programs in mitigating disease spread. Meanwhile, Figure 5(c) reveals a decline in the recovered population, suggesting that fewer individuals progress through the infection due to lower transmission rates. Figure 6 explores the inhibitory effect of preventive measures among susceptible individuals. As the prevention rate k_1 increases with values $k_1 = 0, 0.03, 0.06,$ and 0.08, a stronger inhibition effect is observed, resulting in an increased susceptible population and

decreased infected and recovered populations. This finding underscores the importance of preventive strategies in minimizing disease transmission. Similarly, Figure 7 demonstrates the effect of treatment on infected individuals. As the treatment rate k_2 rises with values $k_2 = 0, 0.3, 0.6$, and 0.8, the inhibition effect strengthens, leading to a growth in the susceptible population while reducing both infected and recovered populations. This highlights the critical role of treatment in limiting disease spread and reducing infection levels. Lastly, Figure 8 examines the impact of vaccination on the susceptible, infected, and recovered populations. Vaccination lowers the number of susceptible individuals by granting immunity, which subsequently reduces the infected population. Additionally, the recovered population increases as more individuals acquire immunity through vaccination, reinforcing its essential role in controlling disease transmission.

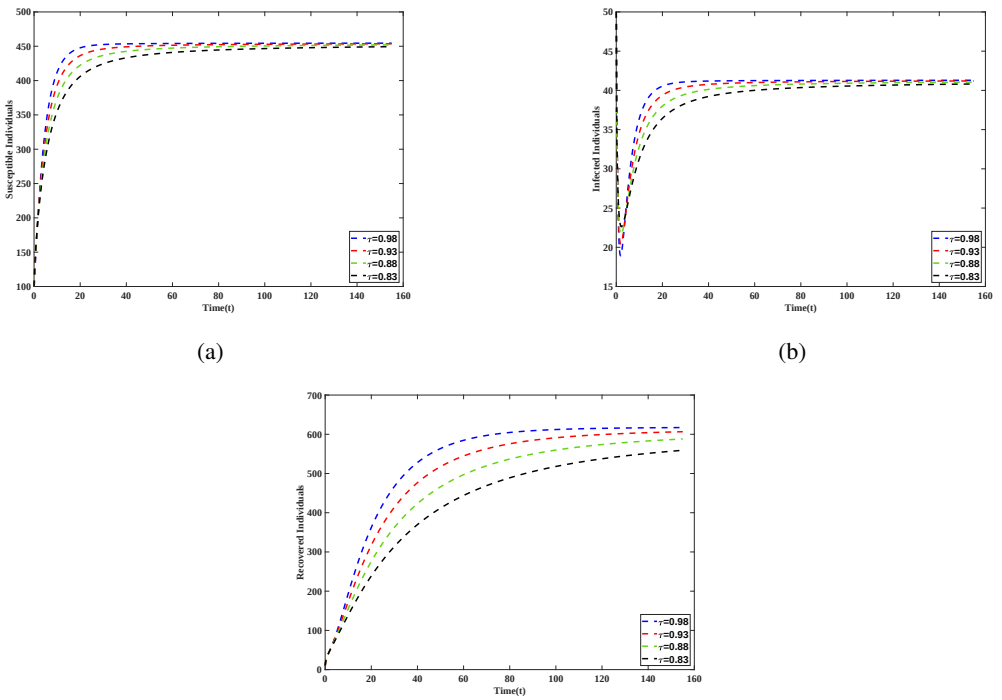

(a) (b)

(c)

Figure 3: The dynamics of the population at different values of parameter τ.

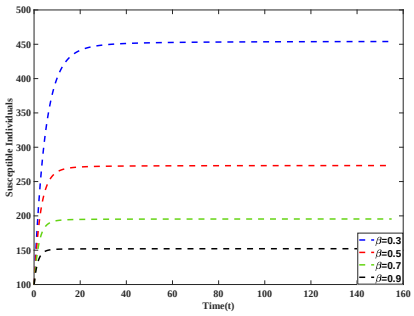

(a)

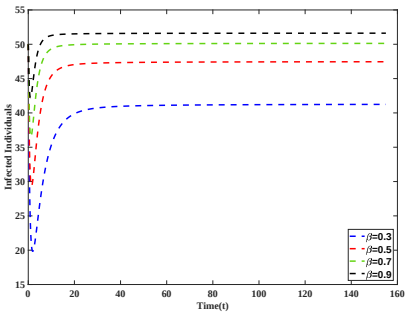

(b)

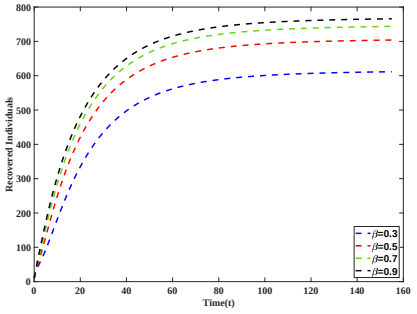

(c)

Figure 4: The dynamics of the population at different values of parameter β.

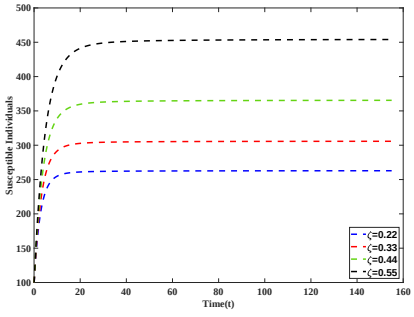

(a)

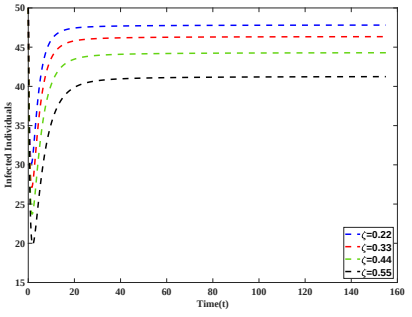

(b)

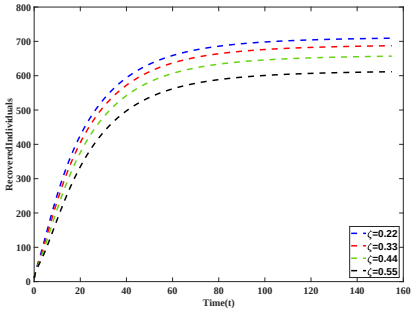

(c)

Figure 5: The dynamics of the population at different values of parameter ζ.

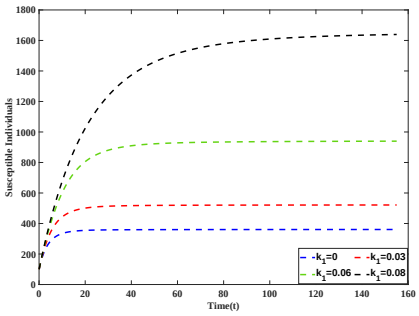

(a)

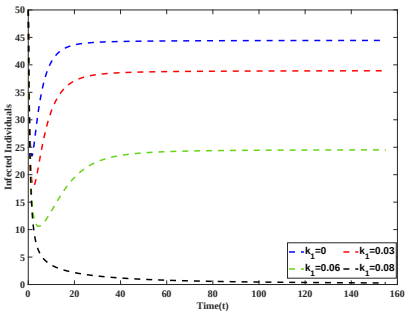

(b)

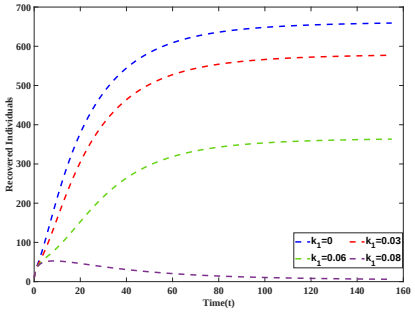

(c)

Figure 6: The dynamics of the population at different values of parameter k_1.

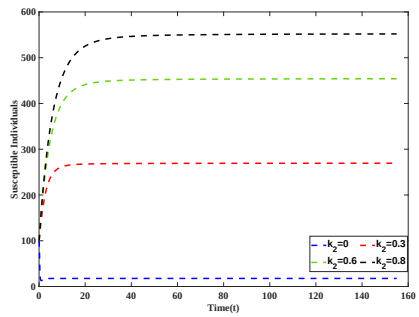

(a)

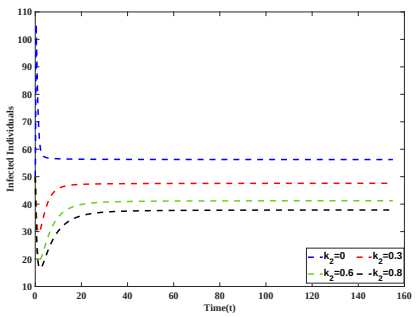

(b)

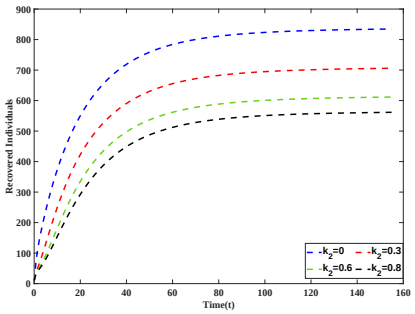

(c)

Figure 7: The dynamics of the population at different values of parameter k_2.

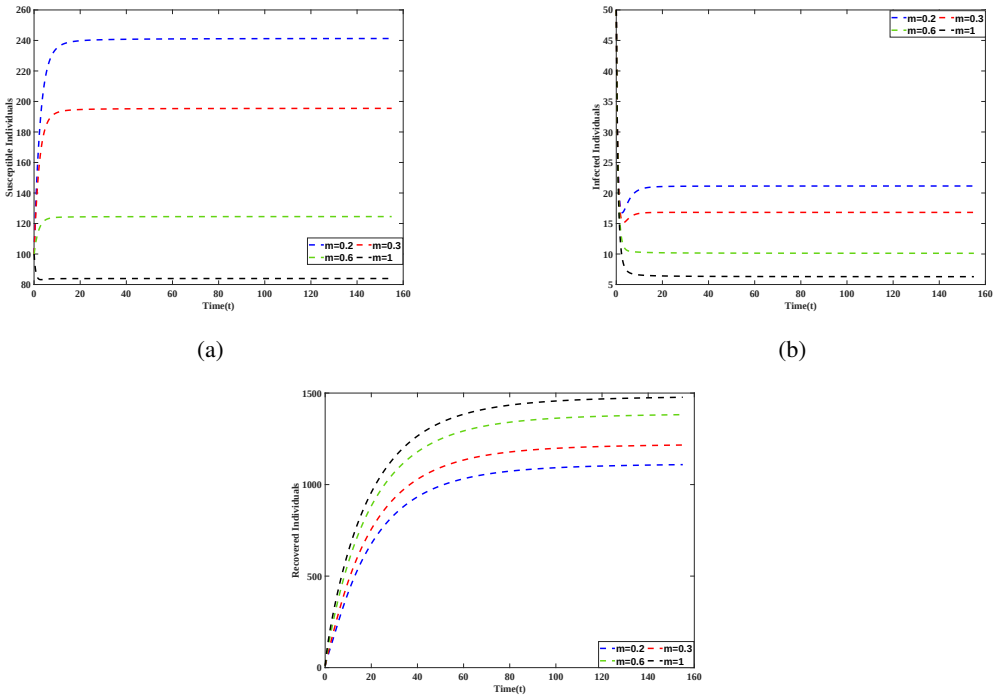

Figure 8: The population dynamics for various values of the parameter $\mathfrak{m}$.

9.2 Comparative table

The comparative analysis between the ABC fractional-order model and the classical ODE model for Hepatitis B highlights key differences in accuracy, stability, and computational behavior. As shown in Table 3, the ABC fractional derivative model demonstrates improved accuracy and greater stability in capturing the memory and hereditary characteristics of the disease. Although the ABC model is computationally more demanding, its ability to more precisely reflect complex disease dynamics makes it a superior choice over the classical model for realistic simulations of Hepatitis B transmission.

Table 3: Comparative analysis of the Fractional model and classical model for all variables over time

	ODE			**Fractional Order** $\mathfrak{a} = 0.98$			**Fractional Order** $\mathfrak{a} = 0.80$		
Time	$\widehat{\mathcal{S}}$	$\widehat{\mathcal{I}}$	$\widehat{\mathcal{R}}$	$\widehat{\mathcal{S}}$	$\widehat{\mathcal{I}}$	$\widehat{\mathcal{R}}$	$\widehat{\mathcal{S}}$	$\widehat{\mathcal{I}}$	$\widehat{\mathcal{R}}$
0	100.00	50.00	10.00	100.00	50.00	10.00	100.00	50.00	10.00
20	451.48	40.93	381.44	447.71	40.54	362.31	395.27	35.44	218.39
40	454.72	41.31	547.45	453.51	41.19	527.97	426.08	38.54	338.39
60	454.75	41.31	598.01	454.04	41.24	584.60	435.96	39.53	410.66
80	454.75	41.31	613.24	454.24	41.26	604.60	440.64	39.98	457.01
100	454.75	41.31	617.83	454.35	41.27	612.09	443.36	40.25	488.41
120	454.75	41.31	619.21	454.42	41.28	615.15	445.15	40.42	510.62
140	454.75	41.31	619.63	454.47	41.29	616.54	446.41	40.54	526.93

10 Discussion and Conclusion

In this study, we developed a FO mathematical model for Hepatitis B using the ABC fractional derivative, which incorporates memory effects due to its non-local and non-singular kernel properties. This method offered a more accurate depiction of disease transmission by considering the long-term influence of past infections on current dynamics. In contrast to traditional models, the fractional-order framework facilitated a deeper understanding of disease progression and control measures. Our model integrated awareness campaigns, vaccination, and a Beddington-DeAngelis type incidence rate to account for preventive strategies and treatment effects. We demonstrated the positivity and boundedness of the system, ensuring that the solutions are biologically meaningful. Additionally, we rigorously established the existence and uniqueness of solutions, confirming the robustness of the model. Stability analysis confirmed both UH and generalized UH stability, ensuring the system's resilience to minor disturbances. Equilibrium analysis revealed two critical equilibrium points: the HBFE and the HBPE. The local asymptotic stability (LAS) of both points was assessed using the basic reproduction number, serving as a threshold for disease persistence or elimination. Moreover, we proved the global asymptotic stability (GAS) of the HBPE using the Lyapunov function, providing strong theoretical validation for the disease's long-term behavior. To understand the effects of various parameters on disease transmission, we performed a sensitivity analysis of the reproduction number, identifying the key factors influencing disease spread. These results are vital for public health strategies, as they pinpoint the parameters that need focused control efforts. To complement our theoretical analysis, we performed numerical simulations using the Lagrange two-step polynomial method, which validated our analytical results and demonstrated the effectiveness of fractional-order modeling. Our findings suggest that increasing awareness programs and effectively implementing the saturation factors (k_1 and k_2) can significantly reduce disease transmission. Sensitivity analysis further indicates that the parameters ζ and k_1 are the most influential in reducing the basic reproduction number.

Future research can extend this model by incorporating optimal control strategies, environmental reservoirs, and co-infections to enhance its applicability. Introducing stochastic effects can provide deeper insights into random fluctuations in disease transmission.

Data availability statement:

Data in a repository
https://archive.cdc.gov/www_cdc_gov/hepatitis/statistics/2018surveillance/HepB.htm

Conflict of Interest Statement

- None of the authors of this paper has a financial or personal relationship with other people or organizations that could inappropriately influence or bias the content of the paper.

- It is to specifically state that "No Competing interests are at stake, and there is no Conflict of Interest" with other people or organizations that could inappropriately influence or bias the content of the paper.

Author contributions

Kaushal Soni: Conceptualization; Investigation; Methodology; Formal analysis; Validation; original draft. Arvind Kumar Sinha: Conceptualization; Investigation; Supervision; Valida tion; Visualization; Writing-review and editing

References

[1] S. Wiersma, *Hepatitis b virus: preventing liver disease with the first vaccine against cancer,* Protect. Against Cancer-Causing Infect, **6**,(2010).

[2] F.A. Wodajo, and T.T. Mekonnen, *Effect of intervention of vaccination and treatment on the transmission dynamics of hbv disease: a mathematical model analysis,* Journal of Mathematics, **2022**, 9968832,(2022).

[3] World health organization, http://www.who.int/mediacentre/factsheets/fs204/en/,(2018).

[4] S.A.A. Shah, M.A. Khan, M. Farooq, S. Ullah, and E.O. Alzahrani, *A fractional order model for hepatitis b virus with treatment via atangana–baleanu derivative,* Physica A: Statistical Mechanics and its Applications, **538**, 122636, (2020).

[5] G.F. Medley, N.A. Lindop, W.J. Edmunds, and D.J. Nokes, *Hepatitis-b virus endemicity: heterogeneity, catastrophic dynamics and control,* Nature medicine, **7(5)**, 619–624, (2001).

[6] B.J. McMahon, *Chronic hepatitis b virus infection* , Medical Clinics, **98(1)**, 39–54, (2014).

[7] J.F. Perz, G.L. Armstrong, L.A. Farrington, Y.J. Hutin, and B.P. Bell, *The contributions of hepatitis b virus and hepatitis c virus infections to cirrhosis and primary liver cancer worldwide,* Journal of hepatology, **45(4)**, 529–538, (2006).

[8] S. Schillie, T.V. Murphy, M. Sawyer, Ly. Kathleen, E. Hughes, R. Jiles, M.A.de Perio, M. Reilly, K. Byrd, and J.W. Ward, *Cdc guidance for evaluating health-care personnel for hepatitis b virus protection and for administering postexposure management,* MMWR Recomm Rep, **62(10)**, 1–19, (2013).

[9] K. Soni, and A.K. Sinha, *Dynamics of epidemic model with conformable fractional derivative*, Nonlinear Science, 100040, (2025).

[10] K. Soni, and A.K. Sinha, *Modeling marburg virus control with limited hospital beds: a fractional approach,* Physica Scripta, **100(1)**, 015251, (2024).

[11] Shyamsunder, and S.D. Purohit, and D. L. Suthar , *A novel investigation of the influence of vaccination on pneumonia disease*, International Journal of Biomathematics, 2450080, (2024).

[12] K. Soni, S. Kumawat, and A.K. Sinha, *Dynamics of marburg virus in the presence of burial and cremation practices: A fractional approach,* Mathematics and Computational Sciences, 2708–2717, (2025).

[13] A.K. Sinha, and Ambika, *Mathematical model of cancer treatment with virotherapy and immune system,* Critical Reviews™ in Biomedical Engineering, **53(3)** 1–11, (2025).

[14] G. Agarwal, M. M. Singh, R. Jan, and S. D. Purohit, *Nonlinear dynamics and stability analysis of a pandemic model using homotopy perturbation,* Critical Reviews™ in Biomedical Engineering, **53(3)** 13–21, (2025).

[15] M.A. Khan and A. Atangana, *Modeling the dynamics of novel coronavirus (2019-ncov) with fractional derivative,* Alexandria Engineering Journal, **59(4)**, 2379–2389, (2020).

[16] A. Abidemi, K.M. Owolabi, and E. Pindza, *Modelling the transmission dynamics of lassa fever with nonlinear incidence rate and vertical transmission,* Physica A: Statistical Mechanics and its Applications, **597**, 127259, (2022).

[17] S. Thornley, C. Bullen, and M. Roberts, *Hepatitis b in a high prevalence new zealand population: a mathematical model applied to infection control policy,* Journal of Theoretical Biology, **254(3)**, 599–603, (2008).

[18] K. Manna, and S.P. Chakrabarty, *Global stability of one and two discrete delay models for chronic hepatitis b infection with hbv dna-containing capsids,* Computational and Applied Mathematics, **36**, 525–536, (2017).

[19] R.M. Anderson, and R.M. May, *Infectious diseases of humans: dynamics and control*, Oxford university press, (1991).

[20] R.M. Anderson, G.F. Medley, and D.J. Nokes, *Preliminary analyses of the predicted impacts of various vaccination strategies on the transmission of hepatitis b virus,* The Control of Hepatitis B: the role of prevention in adolescence, Gower Medical Publishing, London, **274(15)**, 1901–1908, (1992).

[21] J.R. Williams, D.J. Nokes, G.F. Medley, and R.M. Anderson, *The transmission dynamics of hepatitis b in the uk: a mathematical model for evaluating costs and effectiveness of immunization programmes,* Epidemiology & Infection, **116(1)**, 71–89, (1996).

[22] J. Pang, J. A. Cui, and X. Zhou, *Dynamical behavior of a hepatitis b virus transmission model with vaccination,* Journal of Theoretical Biology, **265(4)** , 572–578, (2010).

[23] R. Xu, and Z. Ma., *An hbv model with diffusion and time delay,* Journal of Theoretical Biology, **257(3)** , 499–509, (2009).

[24] M. A. Khan, S. Islam, M. Arif, Z. ul Haq, *Transmission model of hepatitis b virus with the migration effect,* BioMed research international, **2013**, 150681, (2013).

[25] E. Bonyah, S. Ogunlade, S. D. Purohit, and J. Singh, *Modelling cultural hereditary transmission: Insight through optimal control,* Ecological Complexity, **45**, 100890, (2021).

[26] H. Habenom, D. L. Suthar, D. Baleanu, and S.D. Purohit, *A numerical simulation on the effect of vaccination and treatments for the fractional hepatitis b model*. Journal of Computational and Nonlinear Dynamics, **16(1)**, 011004, (2021).

[27] A. Atangana and D. Baleanu, *New fractional derivatives with nonlocal and non-singular kernel: theory and application to heat transfer model,* arXiv preprint arXiv:1602.03408, (2016).

[28] M. Meena, and M. Purohit, *Mathematical analysis using fractional operator to study the dynamics of dengue fever*, Physica Scripta, **99(9)**, 095206, (2024).

[29] S. Kumawat, *Comparative implementation of fractional blood alcohol model by numerical approach*, Critical Reviews in Biomedical Engineering, **53(2)**, 11–19, (2024).

[30] A. Venkatesh, M. Manivel, K. Arunkumar, M. Prakash Raj, Shyamsunder and S.D. Purohit, *A fractional mathematical model for vaccinated humans with the impairment of Monkeypox transmission*, The European Physical Journal Special Topics, 1–21, (2024).

[31] S. Bhatter, K. Jangid, S. Kumawat, D. Baleanu, S. D. Purohit, and D. L. Suthar. *A new investigation on fractionalized modeling of human liver*, Scientific Reports, **14(1)**, 1636, (2024).

[32] M. Aychluh, D. L. Suthar, C. Cesarano and S. D. Purohit, *Modeling and analysis of the dynamics of an excessive gambling problem with modified fractional operator*, An International Journal of Optimization and Control: Theories & Applications, 7096, (2025).

[33] S. Bhatter, S. Kumawat, S. D. Purohit and D. L. Suthar, *Mathematical modeling of tuberculosis using Caputo fractional derivative: a comparative analysis with real data*, Scientific Reports, **15(1)**,12672, (2025).

[34] S. Kumawat, S. Bhatter, B. Bhatia, S. D. Purohit and D. L. Suthar, *Mathematical modeling of allelopathic stimulatory phytoplankton species using fractal–fractional derivatives*, Scientific Reports, **14(1)**,20019, (2024).

[35] S.K. Kushavaha and A. K. Sinha, *Modeling the vertical and horizontal transmission of malaria with intermittent preventive treatment in pregnancy,* SeMA Journal, 1–27, (2024).

[36] M. Moshrefi-Torbati, and J. K.Hammond, *Physical and geometrical interpretation of fractional operators,* Journal of the Franklin Institute, **335(6)**, 1077–1086, (1998).

[37] S. Kumar, R.P. Chauhan, A.A. Aly, S. Momani, and S. Hadid, *A study on fractional hbv model through singular and non-singular derivatives,* The European Physical Journal Special Topics, **231(10)**, 1885–1904, (2022).

[38] J.F. Zhong, N. Gul, R. Bilal, W.F. Xia, M.A. Khan, T. Muhammad, and S. Islam, *A fractal-fractional order atangana-baleanu model for hepatitis b virus with asymptomatic class,* Physica Scripta, **96(7)**, 074001, (2021).

[39] A. Din, and M. Z. Abidin, *Analysis of fractional-order vaccinated hepatitis-b epidemic model with mittag-leffler kernels,* Mathematical Modelling and Numerical Simulation with Applications, **2(2)** , 59–72, (2022).

[40] M. Meena, M. Purohit, S. D. Purohit, and K.S. Nisar , *A novel investigation of the hepatitis B virus using a fractional operator with a non-local kernel*, Partial Differential Equations in Applied Mathematics, **8**, 100577, (2023).

[41] S. Bhatter, and K. Jangid, S.D. Purohit, *A Study Of The Hepatitis B Virus Infection using HIlfer Fractional Derivatives,* Proceedings of Institute of Mathematics & Mechanics National Academy of Sciences of Azerbaijan, **48**, (2022).

[42] M. M. Gour, L. K. Yadav, S. D. Purohit, and D. L. Suthar, *Homotopy decomposition method to analysis fractional hepatitis B virus infection model*, Applied Mathematics in Science and Engineering, **31(1)**, 2260075, (2023).

[43] J. R. Beddington, *Mutual interference between parasites or predators and its effect on searching efficiency,* The Journal of Animal Ecology, 331–340, 1975.

[44] D. L. DeAngelis, R. A. Goldstein, and R.V. O'Neill, *A model for tropic interaction,* Ecology, **56(4)**, 881–892, (1975).

[45] A. Suryanto, W. M. Kusumawinahyu, I. Darti, and I. Yanti, *Dynamically consistent discrete epidemic model with modified saturated incidence rate,* Computational and Applied Mathematics, **32(2)**, 373–383, (2013).

[46] A. Kaddar, *On the dynamics of a delayed sir epidemic model with a modified saturated incidence rate,* Electronic Journal of Differential Equations (EJDE)[electronic only], **2009**, (2009).

[47] M. I. Syam, and M. Al-Refai, *Fractional differential equations with atangana–baleanu fractional derivative: analysis and applications,* Chaos, Solitons & Fractals: X, **2**, 100013, (2019).

[48] W. Sintunavarat, and A. Turab, *Mathematical analysis of an extended seir model of covid-19 using the abc-fractional operator,* Mathematics and Computers in Simulation, **198**, 65–84, (2022).

[49] M. A. Taneco-Hernández, and C. Vargas-De-León, *Stability and lyapunov functions for systems with atangana–baleanu caputo derivative: an hiv/aids epidemic model* Chaos, Solitons & Fractals, **132**, 109586, (2020).

[50] T. Nabil, *Krasnoselskii n-tupled fixed point theorem with applications to fractional nonlinear dynamical system,* Advances in Mathematical Physics, **2019(1)**, 6763842, (2019).

[51] N. I. Okposo, M. O. Adewole, E. N. Okposo, H. I. Ojarikre, and F. A. Abdullah, *A mathematical study on a fractional covid-19 transmission model within the framework of nonsingular and nonlocal kernel,* Chaos, Solitons & Fractals, **152** ,111427, (2021).

[52] A. A. Kilbas, H. M. Srivastava, and J. J. Trujillo, *Theory and applications of fractional differential equations*, Elsevier, **204**, (2006).

[53] O. Diekmann, J. A. P. Heesterbeek, and M. G. Roberts, *The construction of next-generation matrices for compartmental epidemic models,* Journal of the royal society interface, **7(47)**, 873–885, (2010).

[54] Centers for Disease Control and Prevention (CDC), Viral Hepatitis Surveillance Report of Hepatitis B, https://archive.cdc.gov/www_cdc_gov/hepatitis/statistics/2018surveillance/HepB.htm, 2018. Accessed 04 July 2025.

[55] J. E. Solís-Pérez, J. F. Gómez-Aguilar, and A. Atangana, *Novel numerical method for solving variable-order fractional differential equations with power, exponential and mittag-leffler laws,* Chaos, Solitons & Fractals, **114**, 175–185, (2018).

[56] M. Gümüş, and K. Türk, *Dynamical behavior of a hepatitis b epidemic model and its nsfd scheme,* Journal of Applied Mathematics and Computing, **70(4)**, 3767–3788, (2024).

[57] M. B. Sannathimmappa, V. Nambiar, and R. Arvindakshan, , *Hepatitis B: Knowledge and awareness among preclinical year medical students*, Avicenna journal of medicine, **9(02)**, 43–47, (2019).

Author information

Kaushal Soni, Department of Mathematics, National Institute of Technology Raipur, India.
E-mail: kaushalmath2205@gmail.com

Arvind Kumar Sinha, Department of Mathematics, National Institute of Technology Raipur, India.
E-mail: aksinha.maths@nitrr.ac.in

Received: 2025-04-04
Accepted: 2025-07-28